Supporting Information for

A microRNA Network Regulates Expression and Biosynthesis of CFTR and CFTR-ΔF508

Shyam Ramachandran[a,b], Philip H. Karp[c], Peng Jiang[c], Lynda S. Ostedgaard[c], Amy E. Walz[a], John T. Fisher[e], Shaf Keshavjee[h], Kim A. Lennox[i], Ashley M. Jacobi[i], Scott D. Rose[i], Mark A. Behlke[i], Michael J. Welsh[b,c,d,g], Yi Xing[b,c,f], Paul B. McCray Jr.[a,b,c]

Author Affiliations: Department of Pediatrics[a], Interdisciplinary Program in Genetics[b], Departments of Internal Medicine[c], Molecular Physiology and Biophysics[d], Anatomy and Cell Biology[e], Biomedical Engineering[f], Howard Hughes Medical Institute[g], Carver College of Medicine, University of Iowa, Iowa City, IA-52242

Division of Thoracic Surgery[h], Toronto General Hospital, University Health Network, University of Toronto, Toronto, Canada-M5G 2C4

Integrated DNA Technologies[i], Coralville, IA-52241

To whom correspondence should be addressed: Email: michael-welsh@uiowa.edu (M.J.W.); yi-xing@uiowa.edu (Y.X.); Email: paul-mccray@uiowa.edu (P.B.M.)

This PDF file includes:

Fig. S17. Epistatic relationship between SIN3A and miR-138.
Table S1. Expression of microRNAs in human airway epithelia
Table S2. CFTR-Associated Gene Network
Table S3. Enrichment significance for genes influencing CFTR biogenesis
Table S4. Genes in the CFTR-Associated Gene Network identified as differentially expressed in Calu-3 cells following miR-138 or SIN3A DsiRNA treatment
Table S5. Gene Ontology enrichment of genes co-regulated in Calu-3 cells following miR-138 mimic or SIN3A DsiRNA treatment

MATERIALS AND METHODS

Primary Human airway epithelia: Airway epithelia from human trachea and primary bronchus removed from organs donated for research were cultured at the air-liquid interface (ALI) (1). These studies were approved by the Institutional Review Board of the University of Iowa. Briefly, airway epithelial cells were dissociated from native tissue by pronase enzyme digestion. Permeable membrane inserts (0.6 cm^2 Millipore-PCF, 0.33 cm^2 Costar-Polyester) pre-coated with human placental collagen (IV, Sigma) were seeded with freshly dissociated epithelia. Seeding culture media used was DMEM/F-12 medium supplemented with 5% FBS, 50 units/mL penicillin, 50 μg/mL streptomycin, 50 μg/mL gentamicin, 2 μg/mL fluconazole, and 1.25 μg/mL amphotericin B. For epithelia from cystic fibrosis (CF) patients, the following additional antibiotics were used for the first 5 days: 77 μg/mL ceftazidime, 12.5 μg/mL imipenem and cilastatin, 80 μg/mL tobramycin, 25 μg/mL piperacillin and tazobactam. After seeding, the cultures were maintained in DMEM/F-12 medium supplemented with 2% Ultroser G (USG, Pall Biosepra) and the above listed antibiotics.

RNA isolation: Total RNA from human primary airway epithelial cultures, and cell lines (Calu-3, HEK293T, HeLa, CFBE) was isolated using the *mir*Vana™ miRNA isolation kit (Ambion) (2). Total RNA was tested on an Agilent Model 2100 Bioanalyzer (Agilent Technologies). Only samples with an RNA integrity number (RIN) over 7.0 were selected for downstream processing.

TaqMan Low Density microRNA Array (TLDA): Global microRNA (miRNA) expression profiling was performed using the TaqMan® Human MicroRNA Array Set v2.0 (Applied Biosystems), which screens for the expression of 667 human miRNAs plus endogenous controls. Total RNA was isolated from primary cultures (a minimum of 30 days post-seeding) from 4 human non-CF donors, reverse transcribed using the Megaplex™ RT primers, Human Pool Set v2.0 (Applied Biosystems), and quantitated on an Applied Biosystems 7900 HT Real-Time PCR system. The TLDA data were processed using the accompanying software RQ Manager (Applied Biosystems). For each sample, the normalization factor was calculated as a mean of the two endogenous controls, RNU44 and RNU48. ΔC_q was calculated for each miRNA as (C_q(miRNA)-normalization factor). All protocols followed were as per the manufacturer's recommendation.

Oligonucleotide Transfections: Freshly dissociated human airway epithelial cells or immortalized cell lines were transfected in pre-coated 96 well plates (Costar) or Transwell™ Permeable Supports (0.33 cm^2 0.4 μm polyester membrane, Costar 3470). Lipofectamine™ RNAiMAX (Invitrogen) was used as a reverse transfection reagent. Pre-coated (with human placental collagen Type IV, Sigma) substrates were incubated with the transfection mix comprising of Opti-MEM (Invitrogen), oligonucleotide (Integrated DNA Technologies) and Lipofectamine™ RNAiMAX (Invitrogen). 15-20 minutes later, 200,000 freshly dissociated cells suspended in DMEM/F-12 were added to each well/insert. Between 4-6 hrs later, all media from

the apical surface was aspirated and complete media added to the basolateral surface. Media on the basolateral surface were changed every 3-4 days. For human primary epithelial cultures, USG media described above was used. For cultures from immortalized cell lines: Calu-3, CFBE41o- (termed CFBE throughout (3)), complete media specific to each cell line was used (Calu-3: MEM (Gibco) + 10% FBS (Atlanta Biologicals) + 1% Pen Strep (Gibco); CFBE: Advanced DMEM (Gibco) + 1% L-Glutamine (Gibco) + 10% FBS (Atlanta Biologicals) + 1% Pen Strep (Gibco)).

Oligonucleotide reagents: The DsiRNAs were designed (4, 5), synthesized and validated (6, 7) by Integrated DNA Technologies. The miRNA-mimic (6, 8) and anti-miRNA(9, 10) were also designed and synthesized by Integrated DNA Technologies. All accompanying control sequences (Scr) were also generated by Integrated DNA Technologies.
r = RNA
m = 2'OMe modification
SS = Sense strand
AS = Antisense strand
* = Phosphorothioate linkages
+ = Locked Nucleic Acid modification
SpC3 = C3 Spacer modification

SIN3A DsiRNA
Sense strand sequence: /5Phos/rGrCrGrArUrArCrArUrGrArArUrUrCrArGrArUrArCrUrACC
Antisense strand sequence:
/5Phos/rGrGrUrArGrUrArUrCrUmGrAmArUrUrCrArUrGrUmArUmCrGmCmUmC

CFTR DsiRNA
Sense strand sequence: /5Phos/rGrGrArArGrArArUrUrCrUrArUrUrCrUrCrArArUrCrCrAAT
Antisense strand sequence:
/5Phos/rArUrUrGrGrArUrUrGrAmGrAmArUrArGrArArUrUmCrUmUrCmCmUmU

Scr (Negative control for DsiRNAs)
Sense strand sequence: /5Phos/rCrGrUrUrArArUrCrGrCrGrUrArUrArArUrArCrGrCrGrUAT
Antisense strand sequence:
/5Phos/rArUrArCrGrCrGrUrArUmUrAmUrArCrGrCrGrArUmUrAmArCmGmAmC

miR-138 anti-miRNA
mC*mG*+G* mCmC+T mGmA+T mUmC+A mCmA+A mCmA+C mCmA*+G* mC*mU

Scr (negative control for anti-miRNA)
mG*mC*+G* mU*mA*+T* mU*mA*+T* mA*mG*+C* mC*mG*+A* mU*mU*+A* mA*mC*+G* mA

miR-138 mimic
Sense strand sequence: /5SpC3/rCmG rGmC/iSpC3/ mUrGmA rUmUrC mArCmA rAmCrA mCrCmA rGmCrU
Antisense strand sequence: /5Phos/rArG rCrUrG rGrUrG rUrUrG rUrGrA rArUrC rArGrG mCmCmG

Specificity of oligonucleotide transfections: To ascertain the specificity of the following oligonucleotides: CFTR DsiRNA, SIN3A DsiRNA, miR-138 mimic, and miR-138 anti-miRNA, we harvested RNA from cells transfected with these oligonucleotides and measured the expression of multiple genes and miRNAs (SI Fig. S15). 24 hrs post-transfection, RNA was harvested from each sample and subjected to quantitative RT-PCR for the following genes: SFRS9 (normalizer for mRNA), GAPDH, HPRT, RNU48 (normalizer for miRNAs), miRs-21, -24, -26a, -200c, -146a, -146b, -27a*, -134.

Quantitative RT-PCR (RT-qPCR): First-strand cDNA was synthesized using SuperScript® II (Invitrogen), and oligo-dT and random-hexamer primers.Sequence specific PrimeTime® qPCR Assays for human CFTR, SIN3A, GAPDH, HPRT, and SFRS9 were designed and validated (Integrated DNA Technologies). To quantitate miRNAs, TaqMan® microRNA Assays (Applied Biosystems) were obtained for miR-138, RNU48 (control) and 8 other miRNAs (negative control, miRs-21, -24, -26a, -200c, -146a, -146b, -27a*, -134). All reactions were setup using TaqMan® Fast Universal PCR Master Mix (Applied Biosystems) and run on the Applied Biosystems 7900 HT Real-Time PCR system. All experiments were performed in quadruplicate. mRNA and miRNA quantification in cell lines represents 8 independent transfections in 4 separate experiments. mRNA quantification in human primary airway epithelial cultures represent 8 independent transfections in 8 non-CF donors and 4 CF donors.
/56-FAM/: single isomer 6-carboxyfluorescein
/3IABkFQ/: Iowa Black FQ = dark quencher

CFTR:
Forward- CAACATCTAGTGAGCAGTCAGG
Reverse- CCCAGGTAAGGGATGTATTGTG
Probe- /56-FAM/TCCAGATCCTGGAAATCAGGGTTAGT/3IABkFQ/
SIN3A:
Forward- GCACAGAAACCAGTATTTCTCCC
Reverse- GGTCTTCTTGCTGTTTCCTTCC
Probe- /56-FAM/TGCTCTCGACCACGTTGACACTTCC/3IABkFQ/
GAPDH:
Forward- GGCATGGCCTTCCGTGT
Reverse- GCCCAGGATGCCCTTGAG
Probe- /56-FAM/CCTGCTTCACCACCTTCTTGATGTCATCAT/3IABkFQ/
HPRT:
Forward- GACTTTGCTTTCCTTGGTCAG
Reverse- GGCTTATATCCAACACTTCGTGGG
Probe- /56-FAM/ATGGTCAAGGTCGCAAGCTTGCTGGT/3IABkFQ/
SFRS9:
Forward- TGTGCAGAAGGATGGAGT
Reverse- CTGGTGCTTCTCTCAGGATA
Probe- /56-FAM/TGGAATATGCCCTGCGTAAACTGGA/3IABkFQ/
Primers to distinguish between endogenous CFTR and transgene CFTR-HA:
Endogenous CFTR: Forward- AGTGGAGGAAAGCCTTTGGAGT
Endogenous CFTR: Reverse- ACAGATCTGAGCCCAACCTCA
CFTR-HA: Forward- CCCATATGATGTGCCTGATT
CFTR-HA: Reverse- GTCGGCTACTCCCACGTAAA

Electrophysiology studies: Transepithelial Cl^- current measurements were made in Ussing chambers about 2 weeks post-seeding (11). Briefly, primary cultures were mounted in Ussing chambers (EasyMount P2300 chamber system, Physiologic Instruments, San Diego, CA) and voltage clamped (model VCCMC8-4S, Physiologic Instruments), and connected to a computerized data acquisition system (Acquire & Analyze 2.3.181, Physiologic Instruments) to record short-circuit currents and transepithelial resistance. Transepithelial Cl^- current was measured under short-circuit current conditions. Cultures were incubated overnight with 10 μM forskolin and 100 μM 3-isobutyl-1-methylxanthine (IBMX). After measuring baseline current,

the transepithelial current (I_t) response to sequential apical addition of 100 μM amiloride (Amil), 100 μM 4,4'-diisothiocyanoto-stilbene-2,2'-disulfonic acid (DIDS), 4.8 mM [Cl^-], 10 μM forskolin and 100 μM 3-isobutyl-1-methylxanthine (IBMX), and 100 μM GlyH-101 was measured. Studies were conducted with a Cl^- concentration gradient containing 135 mM NaCl, 1.2 mM $MgCl_2$, 1.2 mM $CaCl_2$, 2.4 mM K_2PO_4, 0.6 mM KH_2PO_4, 5 mM dextrose, and 5 mM Hepes (pH 7.4) on the basolateral surface, and gluconate substituted for Cl^- on the apical side. Transepithelial current measurements were made in 24 Calu-3 ALI cultures, 6 each from four independent experiments, pre-transfected with reagents noted; 3 ALI cultures per condition in human primary airway epithelial cultures (*CFTR* Q493X/S912X); 8 ALI cultures per condition in human primary airway epithelia donors (wild-type *CFTR*, *CFTR* ΔF508/ΔF508, *CFTR* ΔF508/3659DC, *CFTR* ΔF508/R1162X). To confirm that the effects of oligonucleotide transfections persisted at the time of conducting the Ussing chamber studies, RT-qPCR and immunoblots measuring SIN3A and CFTR expression in Calu-3 cells (SI Fig. S16A, B) and CFBE cells (SI Fig. S16C) were performed 14 days post-transfection.

Dual-luciferase reporter assay: The 3'UTR of SIN3A was cloned into the Xho1/Not1 restriction enzyme sites in the 3'UTR of *Renilla* luciferase in the psiCHECK™-2 vector (Promega). HEK293T cells were cotransfected with 20ng of psiCHECK-2 vector and different concentrations of miR-138 mimic. The Lipofectamine™ RNAiMAX (Invitrogen) reverse transfection protocol was used as described above. The miR-138 binding sites on the SIN3A 3'UTR were mutated using the site-directed, ligase-independent mutagenesis (SLIM) protocol (12, 13). A plasmid with the scrambled miR-138 binding seed sequence was also cotransfected into HEK293T cells with different concentrations of miR-138 mimic using the Lipofectamine™ RNAiMAX reverse transfection protocol. The Luciferase Assay Reagent (Promega) was used to measure knockdown of *Renilla* luciferase with the SIN3A 3'UTR (wild type or scrambled) downstream in response to the miR-138 mimic. *Renilla* luciferase expression was normalized to firefly luciferase.

SIN3A 3'UTR:
5'-^{1}CUGCAAAG……^{294}**CACCAGCA**……^{726}**CACCAGC**……^{2593}AGGGCUAA-3'
The miR-138 seed sequence binding site on the SIN3A 3'UTR is shown (bold). The nucleotides in bold were mutated to test for sequence specificity of miR-138 mediated repression. The seed sequences were mutated to 5-CUAAUCGC-3'.

Primer sequences to amplify SIN3A 3'UTR:
F- AAGTTTAAACCTGCAAAGCCAGAGC
R- TTGCGGCCGCTTAAGTAAGAACCAAGC
SLIM primers for mutating miR-138 binding sites in the SIN3A 3'UTR:
First miR-138 binding site
FS- GAGCTAAGACTGGAGTCTCC
RS – TGTGCAAGCAAACTGCATGTC
FT-
GTTTGCTTGCACACGTTAATCGAGCTAAGACTGGAGTCTCCTGTGGCCTAACTTTCA
ATG
RT –
CATTGAAAGTTAGGCCACAGGAGACTCCAGTCTTAGCTCGATTAACGTGTGCAAGCA
AAC
Second miR-138 binding site
FS – TTTACTCTCTGACACACACACG

RS – GATGGCACTAAGGTAGAC
FT – GTCTACCTTAGTGCCATCCGTTAATTTTACTCTCTGACACACACACG
RT – CGTGTGTGTGTCAGAGAGTAAAATTAACGGATGGCACTAAGGTAGAC

SDS-PAGE and Immunoblotting: Cell lines or primary cultures were washed with PBS and lysed in freshly prepared lysis buffer (1% Triton, 25mM Tris pH 7.4, 150mM NaCl, protease inhibitors (cOmplete™, mini, EDTA-free, Roche)) for 30 min at 4^{o}C. The lysates were centrifuged at 14,000 rpm for 20 min at 4^{o}C, and the supernatant quantified by BCA Protein Assay kit (Pierce). 20 μg (Calu-3) and 50 μg (human primary airway epithelial cultures, HeLa, HEK293T) of protein per lane was separated on a 7% SDS-PAGE gel for western blot analysis. Antibodies were procured for SIN3A (1:1000, Thermo Scientific), CTCF (1:500, Cell Signaling Technology), CFTR (R-769 (1:2000, CFFT), MM13-4 (1:1000, Millipore), M3A7 (1:500, Millipore), 24-1 (1:1000, R&D Systems)), hemagglutinin (1;1000, Covance) and α-tubulin (1:10000, Sigma). Protein abundance was quantified by densitometry using an AlphaInnotech Fluorochem Imager (AlphaInnotech). For CFTR, band B and C were quantified separately. All bands were normalized to α-tubulin. Experiments were performed in triplicates per donor and mean and standard error of the mean determined using unpaired two-tailed t-test. SIN3A and CFTR immunoblots in cell lines shown represent 8 independent transfections pooled. Densitometry measurements in cell lines represents western blots performed in triplicate from 4 separate experiments. SIN3A and CFTR immunoblots in human primary airway epithelial cultures shown represent 8 independent transfections. Densitometry measurements in human primary airway epithelial cultures represent 8 independent transfections in 8 non-CF donors each and 4 CF donors each. Western blots were probed, stripped and re-probed as follows. PVDF membranes were first probed with the R-769 anti-CFTR antibody. After imaging, the PVDF membrane was stripped with Restore Western Blot Stripping Buffer (Thermo Scientific) for 15 minutes, washed in Tris Buffered Saline-Tween (TBS-T) and blocked in 5% Bovine Serum Albumin (BSA, Pierce) for 1 hr. The membrane was washed in TBS-T and incubated with the goat anti-mouse secondary antibody (1:10000, Sigma) for 1 hr and imaged. If signal was detected, the stripping procedure was repeated till no signal was observed. The membrane was washed in TBS-T, blocked for 1 hr in 5% BSA and re-probed with the M3A7+MM13-4 anti-CFTR antibody cocktail or the anti-HA antibody. The following pairs of western blots were probed with R-769, and re-probed with M3A7+MM13-4): SI Fig. S6B-both panels, Fig. S13B-both panels, Fig. S15E-both panels.

Measuring cell surface display of CFTR: Hela cells stably expressing wild-type CFTR or CFTR-ΔF508 were kindly provided by Dr. G. Lukacs (14, 15). Cell surface ELISA was performed on these cells (16) 6 hrs, 12 hrs, and 24 hrs after transfecting with oligonucleotides. HeLa cells were transfected in 96 well plates (Costar) with the SIN3A DsiRNA and miR-138 mimic as described earlier using the Lipofectamine™ RNAiMAX (Invitrogen) recommended reverse transfection protocol. Briefly, the plate containing the cells was moved to a cold room (4^{o}C), and all media used was ice cold. Cells were washed with PBS, and blocked for 30 min with PBS containing 5% BSA. Anti-HA primary antibody (Covance) was added in 5% BSA-PBS at a 1:1000 concentration for 1 hr. Cells were washed with PBS, and anti-mouse secondary antibody HRP conjugated (Amersham) was added to cells at 1:1000 concentration in 5% BSA-PBS for 1 hr. Cells were washed through, and signal developed using SureBlue Reserve™ TMB Microwell Substrate (KPL). The reaction was stopped and read on a VersaMax™ Microplate Reader (Molecular Devices) at 540 nm using the SoftMax® Prof Software (Molecular Devices). For normalization, cells were lysed and total protein quantitated using the BCA Protein Assay kit (Pierce). The experiment was performed in quadruplicate, and the data presented as a mean ±

standard deviation of individual data points. Statistical significance between groups was determined using Student's t-test.

Transduction of human primary airway epithelial cultures: Primary airway epithelial cell cultures were transduced with an adenovirus expressing either wild-type CFTR or CFTR-ΔF508 (17, 18) at a MOI of 100. The primary culture insert was inverted, the virus was suspended in 50 µl of DMEM, and added to the basolateral surface of the culture for a period of 4 hrs. The similar step was then repeated for the apical surface. Throughout, the cultures were kept at 37^{o}C in a 5% CO_2 incubator. For primary airway epithelial cultures from the CF donor (*CFTR* Q493X/S912X) transfected with oligonucleotides, transduction with the Ad-CFTR-ΔF508 was performed 11 days post-seeding. CFTR immunoblot, RT-qPCR and transepithelial current (I_t) measurements were made 14 days post-seeding.

Microarrays: Calu-3 cells were transfected with SIN3A DsiRNA and miR-138 mimic by reverse transfection as described above. Total RNA was isolated 48 hrs after transfection using the *mir*Vana™ miRNA isolation kit (Ambion), and only samples that had a RIN >7.0 were selected for microarray analysis. Microarrays were performed at the University of Iowa DNA Core (2). Briefly, RNA samples were processed with the NuGEN WT-Ovation™ Pico RNA Amplification System, v1.0 along with the WT-Ovation™ Exon Module, v1.0 (NuGEN Technologies) according to the manufacturer's recommended protocols. The GeneChip® Human Exon 1.0 ST Array (Affymetrix) was used to probe the samples. Arrays were scanned using the Affymetrix Model 3000 (7G) scanner and the data collected using the GeneChip® Operating Software (GCOS), v.1.4. Data analysis was performed on Partek® Genomics Suite™ (Partek) using the one-way ANOVA and Student's t-test to determine differentially expressed genes.

Iodide Efflux assay: Iodide efflux measurements in HeLa cells were made using a protocol adapted by Lukacs and colleagues (14, 19). Briefly, HeLa cells were transfected with oligonucleotides in 24 well plates (Costar), and the assay was performed 48 hrs post-transfection (8 wells per condition). As controls, HeLa cells stably expressing wild-type CFTR were plated in 24 well plates (4 wells for cAMP induction and 4 wells for DMSO mock). Cells were observed prior to the experiment to ensure ~90% confluence. Wells were washed thrice with 2 ml loading buffer, and incubated in 2 ml loading buffer for 1hr. Wells were washed 7 times in 5 min with 200 µl efflux buffer. 200 µl of efflux buffer was added to each well with a repeat pippetor, and aspirated after 30 sec and stored. After 8 minutes, wells designated for the DMSO control received efflux buffer containing DMSO. Wells designated as test received efflux buffer containing 10 µM forskolin and 100 µM IBMX. 12 such washes were performed in as many minutes. Iodide concentrations in the samples stored were read using iodide selective electrodes that were calibrated with a standard curve.

Chromatin Immunoprecipitation (ChIP): ChIP was carried out using the EZ-ChIP kit from Millipore (Upstate Protocol). Human primary airway epithelial cells were grown on 150 mm dishes and 5 x 10^7 cells were used. Cells were crosslinked with 1% formaldehyde for 10 min and reaction stopped with 0.125 M glycine. Cells were washed with PBS and lysed in 1 ml of 1% SDS, 10 mM EDTA, 50 mM Tris/HCl (pH 8.1) with protease inhibitors. Sample was sonicated to generate fragments under 500 bp. Immunoprecipitation was performed overnight at 4^{o}C with the SIN3A antibody (Santa Cruz Biotechnology). Manufacturer's recommended protocol were followed with modifications (20-23) and immunoprecipitation from each donor was performed in triplicate. Primer sequences used for amplifying DNase I hypersensitive sites (DHS) regions 17a DHS (normalizer), -20.9 DHS, +6.8 DHS and +15.6 DHS (negative control) were obtained

from the literature (20, 21). Intron 17a DHS has been reported to not have a putative CTCF binding site or bind CTCF (20, 21). -20.9 DHS, +6.8 DHS and +15.6 DHS have been shown to have a putative CTCF binding site, but CTCF has been demonstrated to bind only the -20.9 DHS and +6.8 DHS (20, 21). Additional controls used were: co-immunoprecipitation of CTCF with an anti-SIN3A antibody (24), ChIP with anti-SIN3A antibody without formaldehyde crosslinking, and ChIP without the use of anti-SIN3A antibody. As a positive control, ChIP with anti-CTCF antibody was performed and enrichment was confirmed at -20.9 kb relative to 17a.

DHS17A
Forward- GGATAGTGCTGCTATTACTAAAGGTTTCT
Reverse- ATGGCAGCTCCAACACATGA
Probe- /56-FAM/TCTGAAGACAACAAGCCAAAGGGACAAATTT/3IABkFQ/
DHS -20.9
Forward- CCGGGATGTTGTTTGAAGCTT
Reverse- TTTAAATAGTTGAATAGAGGACGAGATACTTT
Probe- /56-FAM/ATAGTATTTTCTTCTCTCTTCCTTACCTGCCCTCTGCT/3IABkFQ/
DHS +15.6
Forward- ATCCATTTTCTTCAAGTCTCTCTCCAT
Reverse- GGAATGAGGATTGTTTATGATTTG
Probe- /56-FAM/CCTCTTTATGGAATCTCCTTTTGATTTGAACTTTGA/3IABkFQ/
DHS +6.8
Forward- TCTTCTTTCCCATTCACCTTTGTC
Reverse- TTTTGGTTTCATTTATACGCACATC
Probe- /56-FAM/CCATTGCTGATAAAGATTGCTCCTTCTATTATTCCA/3IABkFQ/

CFTR-Associated Gene Network: Gene products shown previously to interact with CFTR were curated from published literature (16, 25-27) and were collated to generate a list of CFTR-associated genes. The complete gene list is presented in SI Table S2. This list was cross referenced with the differentially expressed genes from the miR-138 mimic or SIN3A DsiRNA intervention in Calu-3 cells and used to assess the enrichment significance for genes influencing CFTR biogenesis. The complete enrichment profile is available in SI Table S3.

LDH cytotoxicity assay: Calu-3 cells and CFBE cells were transfected with the following reagents- miR-138 mimic, miR-138 anti-miR, SIN3A DsiRNA, CFTR DsiRNA, and Scr. Cells were seeded onto pre-coated filters. The apical surface was washed, and the basolateral media collected on days 4, 8, 12 and 16 post-transfection. LDH cytotoxicity assay kit (Cayman chemical) was used to measure the levels of lactate dehydrogenase in the washes and basolateral media. Percentage toxicity and viability were computed based on LDH levels. Data were normalized to untransfected cells and are presented in SI Fig. S14.

Epistatic relationship between SIN3A and miR-138: HEK293T and Calu-3 cells were transfected with the following reagents: miR-138 mimic/anti-miR, Scr (mimic/anti-miR/DsiRNA), SIN3A DsiRNA, human SIN3A cDNA expression plasmid (CMV driven cassette, OriGene, RC227622), or empty expression plasmid, using lipofectamine RNAiMAX by reverse transfection (Fig. S17). The plasmid transfection efficiency for Calu-3 cells was 20-40% based on a GFP reporter control.

Statistical Analysis: Data are presented as a mean ± standard error of individual data points. Statistical significance between groups was determined using Student's t-test or one-way ANOVA as indicated. A P-value <0.05 was considered significant.

REFERENCES

1. Karp PH*, et al.* (2002) An in vitro model of differentiated human airway epithelia. Methods for establishing primary cultures. *Methods Mol Biol* 188:115-137.
2. Ramachandran S, Clarke LA, Scheetz TE, Amaral MD, & McCray PB, Jr. (2011) Microarray mRNA expression profiling to study cystic fibrosis. *Methods Mol Biol* 742:193-212.
3. Kunzelmann K, *et al.* (1993) An immortalized cystic fibrosis tracheal epithelial cell line homozygous for the delta F508 CFTR mutation. *Am J Respir Cell Mol Biol* 8:522-529.
4. Kim DH*, et al.* (2005) Synthetic dsRNA Dicer substrates enhance RNAi potency and efficacy. *Nat Biotechnol* 23(2):222-226.
5. Rose SD*, et al.* (2005) Functional polarity is introduced by Dicer processing of short substrate RNAs. *Nucleic Acids Res* 33(13):4140-4156.
6. Behlke MA (2008) Chemical modification of siRNAs for in vivo use. *Oligonucleotides* 18(4):305-319.
7. Collingwood MA*, et al.* (2008) Chemical modification patterns compatible with high potency dicer-substrate small interfering RNAs. *Oligonucleotides* 18(2):187-200.
8. Henry JC, Azevedo-Pouly AC, & Schmittgen TD (2011) microRNA Replacement Therapy for Cancer. *Pharm Res* 28(12):3030-3042.
9. Lennox KA & Behlke MA (2011) Chemical modification and design of anti-miRNA oligonucleotides. *Gene Ther* 18(12):1111-1120.
10. Melkman-Zehavi T*, et al.* (2011) miRNAs control insulin content in pancreatic beta-cells via downregulation of transcriptional repressors. *The EMBO journal* 30(5):835-845.
11. Itani OA*, et al.* (2011) Human cystic fibrosis airway epithelia have reduced Cl- conductance but not increased Na+ conductance. *Proc Natl Acad Sci U S A* 108(25):10260-10265.
12. Chiu J, Tillett D, Dawes IW, & March PE (2008) Site-directed, Ligase-Independent Mutagenesis (SLIM) for highly efficient mutagenesis of plasmids greater than 8kb. *J Microbiol Methods* 73(2):195-198.
13. Chiu J, March PE, Lee R, & Tillett D (2004) Site-directed, Ligase-Independent Mutagenesis (SLIM): a single-tube methodology approaching 100% efficiency in 4 h. *Nucleic Acids Res* 32(21):e174.
14. Sharma M, Benharouga M, Hu W, & Lukacs GL (2001) Conformational and temperature-sensitive stability defects of the delta F508 cystic fibrosis transmembrane conductance regulator in post-endoplasmic reticulum compartments. *J Biol Chem* 276(12):8942-8950.
15. Sharma M*, et al.* (2004) Misfolding diverts CFTR from recycling to degradation: quality control at early endosomes. *J Cell Biol* 164(6):923-933.
16. Okiyoneda T*, et al.* (2010) Peripheral protein quality control removes unfolded CFTR from the plasma membrane. *Science* 329(5993):805-810.
17. Zabner J, Zeiher BG, Friedman E, & Welsh MJ (1996) Adenovirus-mediated gene transfer to ciliated airway epithelia requires prolonged incubation time. *J Virol* 70(10):6994-7003.
18. Sinn PL, Shah AJ, Donovan MD, & McCray PB, Jr. (2005) Viscoelastic gel formulations enhance airway epithelial gene transfer with viral vectors. *Am J Respir Cell Mol Biol* 32(5):404-410.
19. Glozman R*, et al.* (2009) N-glycans are direct determinants of CFTR folding and stability in secretory and endocytic membrane traffic. *J Cell Biol* 184(6):847-862.

20. Blackledge NP, *et al.* (2007) CTCF mediates insulator function at the CFTR locus. *Biochem J* 408(2):267-275.
21. Blackledge NP, Ott CJ, Gillen AE, & Harris A (2009) An insulator element 3' to the CFTR gene binds CTCF and reveals an active chromatin hub in primary cells. *Nucleic Acids Res* 37(4):1086-1094.
22. Das PM, Ramachandran K, vanWert J, & Singal R (2004) Chromatin immunoprecipitation assay. *Biotechniques* 37(6):961-969.
23. Fowler AM, Solodin NM, Valley CC, & Alarid ET (2006) Altered target gene regulation controlled by estrogen receptor-alpha concentration. *Mol Endocrinol* 20(2):291-301.
24. Lutz M, *et al.* (2000) Transcriptional repression by the insulator protein CTCF involves histone deacetylases. *Nucleic Acids Res* 28(8):1707-1713.
25. Hutt DM, *et al.* (2010) Reduced histone deacetylase 7 activity restores function to misfolded CFTR in cystic fibrosis. *Nat Chem Biol* 6(1):25-33.
26. Liekens AM, *et al.* (2011) BioGraph: unsupervised biomedical knowledge discovery via automated hypothesis generation. *Genome Biol* 12(6):R57.
27. Wang X, *et al.* (2006) Hsp90 cochaperone Aha1 downregulation rescues misfolding of CFTR in cystic fibrosis. *Cell* 127(4):803-815.
28. Gomes-Alves P, Neves S, Coelho AV, & Penque D (2009) Low temperature restoring effect on F508del-CFTR misprocessing: A proteomic approach. *J Proteomics* 73(2):218-230.
29. Rebhan M, Chalifa-Caspi V, Prilusky J, & Lancet D (1998) GeneCards: a novel functional genomics compendium with automated data mining and query reformulation support. *Bioinformatics* 14(8):656-664.
30. Rebhan M, Chalifa-Caspi V, Prilusky J, & Lancet D (1997) GeneCards: integrating information about genes, proteins and diseases. *Trends Genet* 13(4):163.
31. Safran M, *et al.* (2010) GeneCards Version 3: the human gene integrator. *Database (Oxford)* 2010:baq020.
32. Morito D, *et al.* (2008) Gp78 cooperates with RMA1 in endoplasmic reticulum-associated degradation of CFTRDeltaF508. *Mol Biol Cell* 19(4):1328-1336.
33. Gomes-Alves P, Couto F, Pesquita C, Coelho AV, & Penque D (2010) Rescue of F508del-CFTR by RXR motif inactivation triggers proteome modulation associated with the unfolded protein response. *Biochim Biophys Acta* 1804(4):856-865.
34. Riordan JR (2008) CFTR function and prospects for therapy. *Annu Rev Biochem* 77:701-726.
35. Okiyoneda T, *et al.* (2002) Calnexin Delta 185-520 partially reverses the misprocessing of the Delta F508 cystic fibrosis transmembrane conductance regulator. *FEBS letters* 526(1-3):87-92.
36. Okiyoneda T, *et al.* (2004) Delta F508 CFTR pool in the endoplasmic reticulum is increased by calnexin overexpression. *Mol Biol Cell* 15(2):563-574.
37. Amaral MD (2005) Processing of CFTR: traversing the cellular maze--how much CFTR needs to go through to avoid cystic fibrosis? *Pediatr Pulmonol* 39(6):479-491.
38. Averna M, *et al.* (2011) Calpain digestion and HSP90-based chaperone protection modulate the level of plasma membrane F508del-CFTR. *Biochim Biophys Acta* 1813(1):50-59.
39. Xu Y, Liu C, Clark JC, & Whitsett JA (2006) Functional genomic responses to cystic fibrosis transmembrane conductance regulator (CFTR) and CFTR(delta508) in the lung. *J Biol Chem* 281(16):11279-11291.
40. Rennolds J, *et al.* (2008) Cystic fibrosis transmembrane conductance regulator trafficking is mediated by the COPI coat in epithelial cells. *J Biol Chem* 283(2):833-839.

41. Fu L*, et al.* (2011) Dab2 is a Key Regulator of Endocytosis and Post-endocytic Trafficking of the Cystic Fibrosis Transmembrane Conductance Regulator. *Biochem J* 441(2):633-643.
42. Sun F*, et al.* (2006) Derlin-1 promotes the efficient degradation of the cystic fibrosis transmembrane conductance regulator (CFTR) and CFTR folding mutants. *J Biol Chem* 281(48):36856-36863.
43. Loo MA*, et al.* (1998) Perturbation of Hsp90 interaction with nascent CFTR prevents its maturation and accelerates its degradation by the proteasome. *The EMBO journal* 17(23):6879-6887.
44. McLellan CA, Raynes DA, & Guerriero V (2003) HspBP1, an Hsp70 cochaperone, has two structural domains and is capable of altering the conformation of the Hsp70 ATPase domain. *J Biol Chem* 278(21):19017-19022.
45. Caohuy H, Jozwik C, & Pollard HB (2009) Rescue of DeltaF508-CFTR by the SGK1/Nedd4-2 signaling pathway. *J Biol Chem* 284(37):25241-25253.
46. Yoo JS*, et al.* (2002) Non-conventional trafficking of the cystic fibrosis transmembrane conductance regulator through the early secretory pathway. *J Biol Chem* 277(13):11401-11409.
47. Wang X*, et al.* (2004) COPII-dependent export of cystic fibrosis transmembrane conductance regulator from the ER uses a di-acidic exit code. *J Cell Biol* 167(1):65-74.
48. Wang X, Koulov AV, Kellner WA, Riordan JR, & Balch WE (2008) Chemical and biological folding contribute to temperature-sensitive DeltaF508 CFTR trafficking. *Traffic* 9(11):1878-1893.
49. Yamaguchi A*, et al.* (1999) Stress-associated endoplasmic reticulum protein 1 (SERP1)/Ribosome-associated membrane protein 4 (RAMP4) stabilizes membrane proteins during stress and facilitates subsequent glycosylation. *J Cell Biol* 147(6):1195-1204.
50. Younger JM*, et al.* (2004) A foldable CFTR{Delta}F508 biogenic intermediate accumulates upon inhibition of the Hsc70-CHIP E3 ubiquitin ligase. *J Cell Biol* 167(6):1075-1085.
51. Huang da W, Sherman BT, & Lempicki RA (2009) Bioinformatics enrichment tools: paths toward the comprehensive functional analysis of large gene lists. *Nucleic Acids Res* 37(1):1-13.

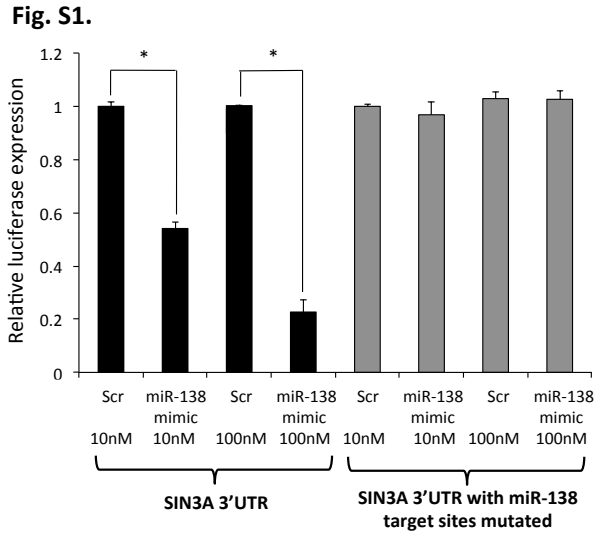

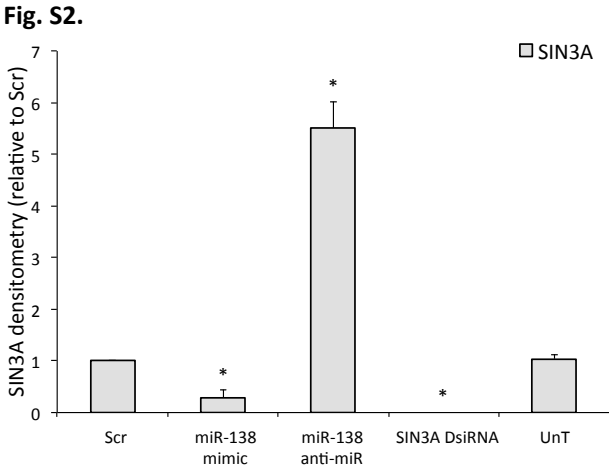

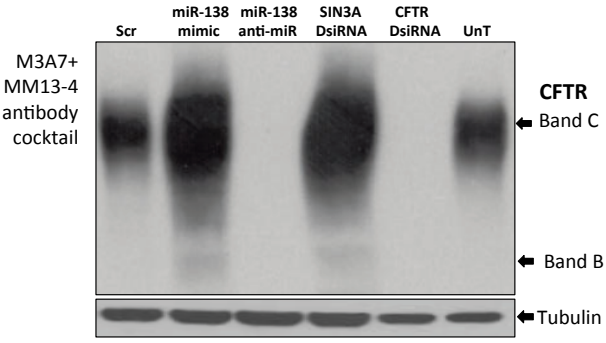

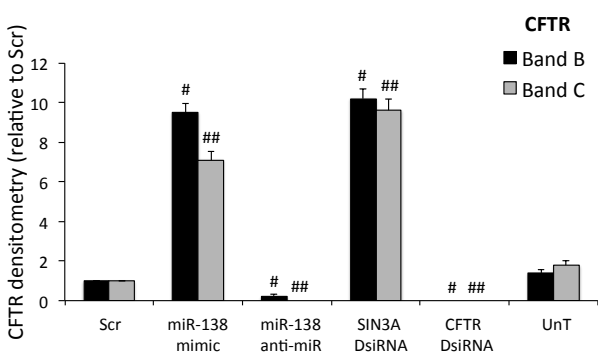

Fig. S1. miR-138 regulates SIN3A in a dose-dependent and site-specific manner. HEK293T cells were co-transfected with the psiCHECK-2 vector (containing the SIN3A 3'UTR) and increasing concentrations of Scr or miR-138 mimic (Scr: non-targeting control oligonucleotide). To test site-specificity, the two predicted binding sites of miR-138 on SIN3A 3'UTR cloned in the psiCHECK-2 vector were mutated and the experiment repeated. Error bars indicate mean ± SE; (n=4, 3 replicates each); **P* <0.01, relative to Scr.

Fig. S2. miR-138 regulates endogenous SIN3A protein expression. Densitometry and relative fold change of SIN3A protein abundance in 6 human donors of primary airway epithelial cultures (8 replicates each). Immunoblots were performed 72 hrs post-transfection. SIN3A DsiRNA (positive control), UnT (Un-transfected cells). Error bars indicate mean ± SE, **P* <0.01, relative to Scr.

Fig. S3. miR-138 regulates endogenous CFTR protein expression in Calu-3 cells. (*A*) Representative CFTR immunoblot in Calu-3 cells 72 hrs post-transfection (M3A7+MM13-4 antibody cocktail). (*B*) Densitometry and relative fold change of CFTR protein abundance (R769 antibody) from (n=4, 3 replicates each). Error bars indicate mean ± SE, $^{\#}P$ <0.01, relative to Scr CFTR band B; $^{\#\#}P$ <0.01, relative to Scr CFTR band C.

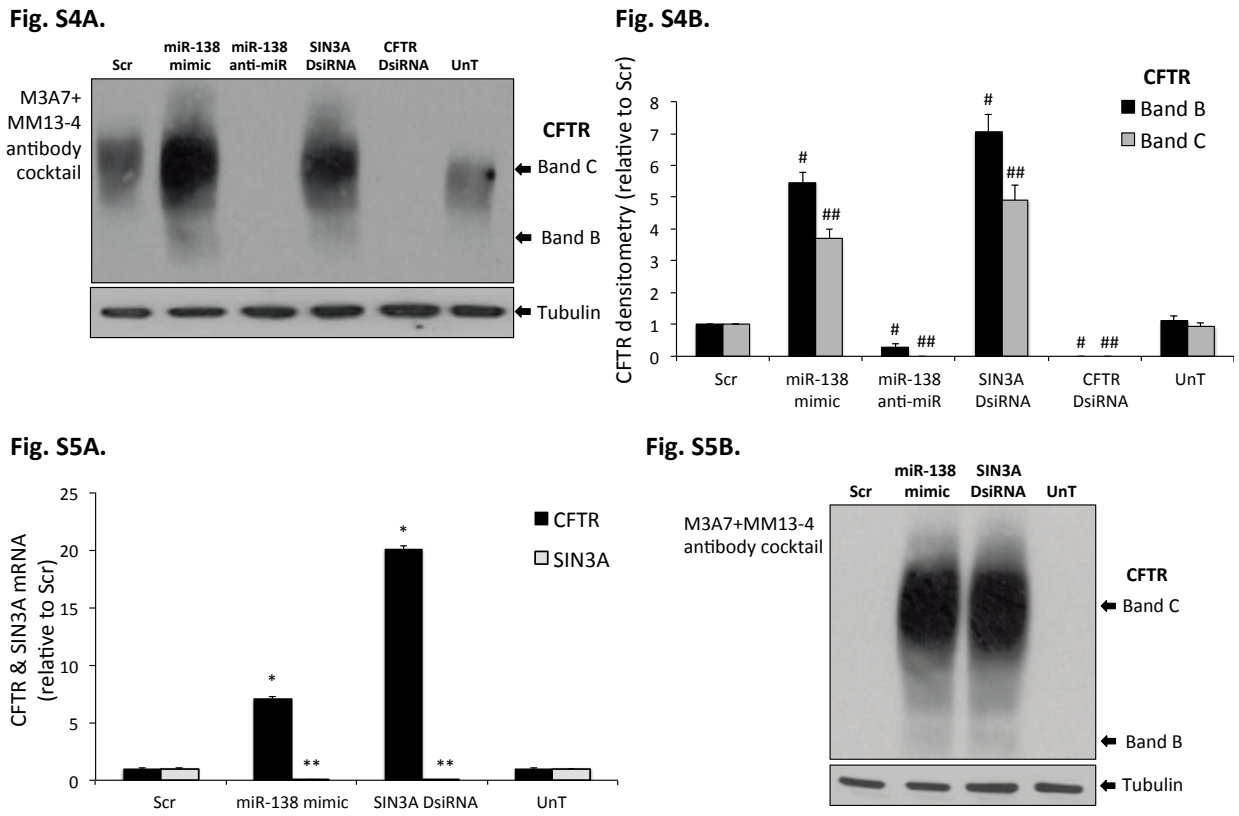

Fig. S4. miR-138 regulates endogenous CFTR protein expression in primary human airway epithelia. (*A*) CFTR immunoblot from one human donor of primary airway epithelial 72 hrs post-transfection (M3A7+MM13-4 antibody cocktail). (*B*) Densitometry and relative fold change of CFTR protein abundance (R769 antibody) in primary airway epithelia from 6 different human donors (8 replicates each). Error bars indicate mean ± SE, $^{\#}P$ <0.01, relative to Scr CFTR Band B; $^{\#\#}P$ <0.01, relative to Scr CFTR Band C.

Fig. S5. miR-138 regulates CFTR expression in HeLa cells. (*A*) Relative *CFTR* and *SIN3A* mRNA abundance in HeLa cells 24 hrs post-transfection (n=4, 8 replicates each). (*B*) Representative CFTR immunoblot (n=4, 3 replicates each) performed 72 hrs post-transfection (M3A7+MM13-4 antibody cocktail). Densitometry not shown as no CFTR protein detected in HeLa cells. Error bars indicate mean ± SE, $*P$ <0.01, relative to Scr (for CFTR); $**P$ <0.01, relative to Scr (for SIN3A).

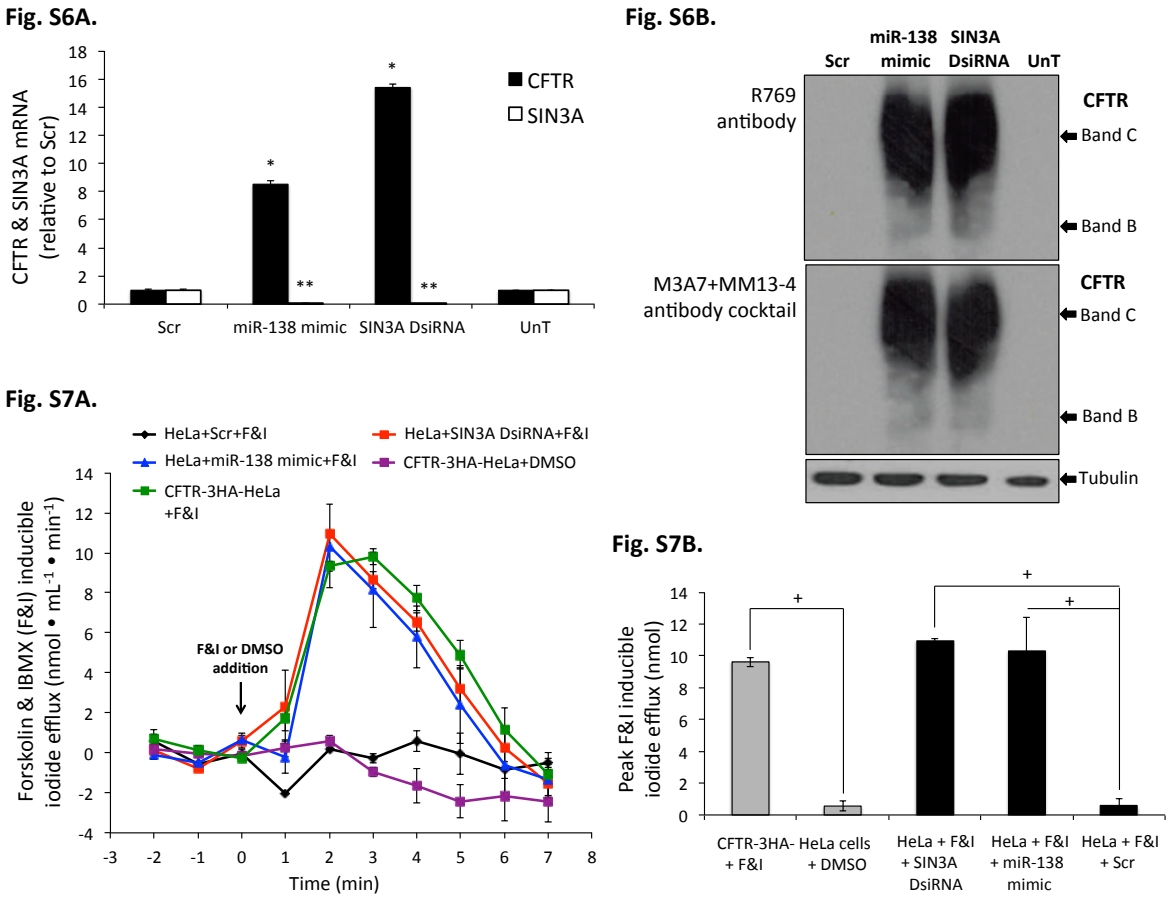

Fig. S6. miR-138 regulates CFTR expression in HEK293T cells. (*A*) Relative *CFTR* and *SIN3A* mRNA abundance in HEK293T cells 24 hrs post-transfection (n=4, 8 replicates each). (*B*) Representative CFTR immunoblots (done in triplicate from 4 separate experiments) performed 72 hrs post-transfection. PVDF membrane was first probed with R769 antibody (top panel), stripped and re-probed with the M3A7+MM13-4 antibody cocktail (bottom panel). Densitometry not shown as no CFTR protein detected in HEK293T cells. Error bars indicate mean ± SE, **P* <0.01, relative to Scr (CFTR); ***P* <0.01, relative to Scr (SIN3A).

Fig. S7. HeLa cells exhibit CFTR channel activity. (*A* and *B*) Iodide efflux assay performed in HeLa cells 48 hrs post-transfection with the miR-138 mimic and SIN3A DsiRNA (8 independent transfections per condition). HeLa cells stably expressing the wild-type CFTR (CFTR-3HA-HeLa) were used as controls. Each data point represents 8 transfections. ^{+}P <0.01. F&I denotes addition of forskolin and IBMX as described in Methods.

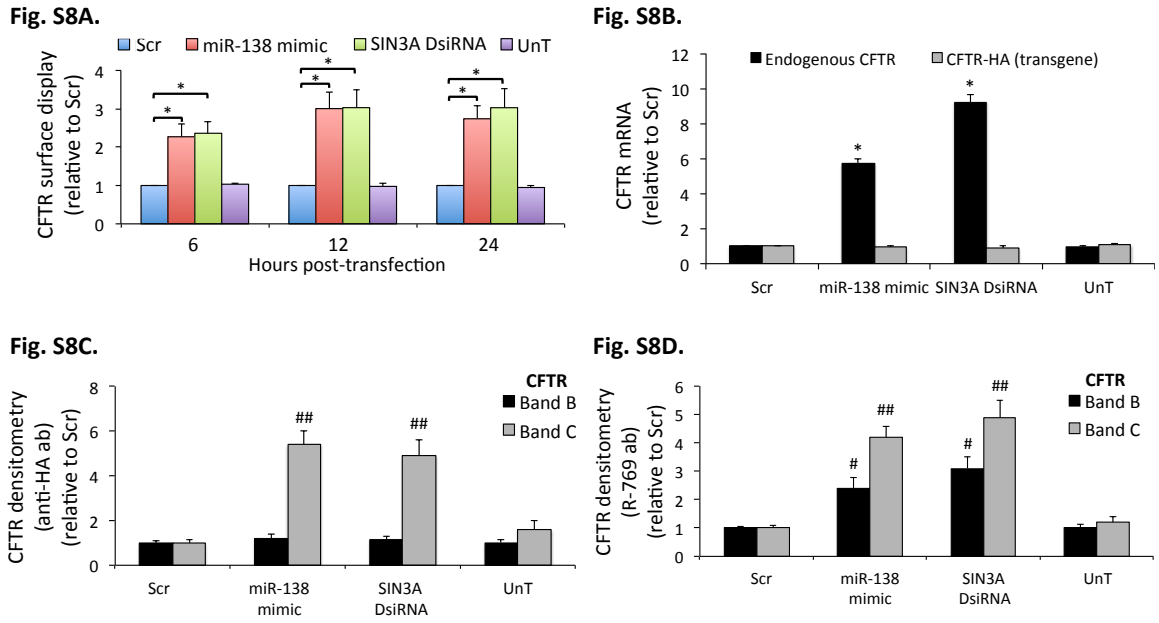

Fig. S8. miR-138 improves CFTR processing. (*A*) Cell surface ELISA to detect CFTR with an anti-HA antibody in HeLa-CFTR cells 6, 12, and 24 hrs post-transfection with noted reagents (n=3, 6 replicates each). (*B*) Relative *CFTR* mRNA abundance in Hela-CFTR cells 24 hrs post-transfection. Primers were designed to distinguish between endogenous *CFTR* mRNA and the CFTR-HA transgene (n=3, 6 replicates each). (*C* and *D*) Densitometry and relative fold change of CFTR protein abundance (n=4, 8 replicates each) in HeLa cells stably expressing the wild type CFTR-3HA. (*C*) Anti-HA antibody (Covance). (*D*) Anti-CFTR antibody (R769 antibody). Based on results in HeLa cells (Fig. 2E, SI Fig. S5) and the increase in endogenous *CFTR* mRNA (SI Fig. S8B) in response to miR-138 mimic or SIN3A DsiRNA, the increased abundance of CFTR band C represents the sum of both CFTR-3HA biogenesis and endogenous CFTR protein expression. Error bars indicate mean ± SE; $^{*}P$ <0.01 relative to Scr; $^{\#}P$ <0.01, relative to Scr CFTR band B; $^{\#\#}P$ <0.01, relative to Scr CFTR band C.

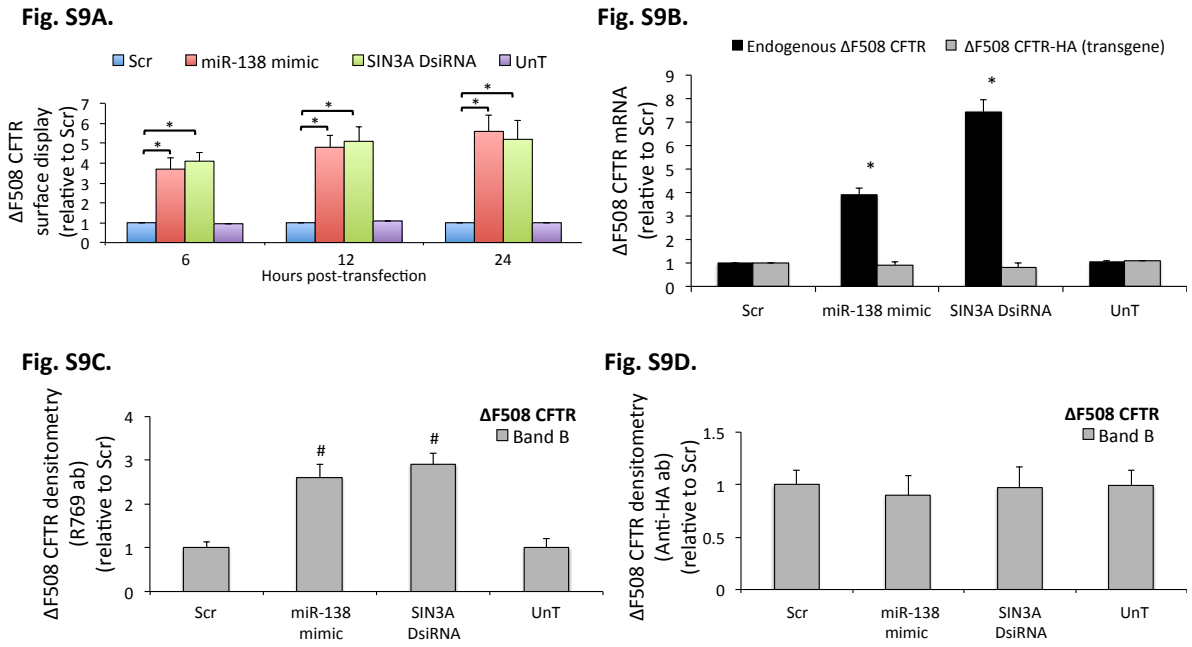

Fig. S9. miR-138 improves CFTR-ΔF508 processing. (*A*) Cell surface ELISA to detect CFTR-ΔF508 with an anti-HA antibody in HeLa-CFTR-ΔF508 cells 6, 12 and 24 hrs post-transfection with noted reagents (n=3, 6 replicates each). (*B*) Relative *CFTR* mRNA abundance in Hela-CFTR cells 24 hrs post-transfection. Primers were designed to distinguish between endogenous *CFTR* mRNA and the CFTR-HA transgene (n=3, 6 replicates each). (*C* and *D*) Densitometry and relative fold change of CFTR-ΔF508 protein abundance (n=4, 8 replicates each) in HeLa cells stably expressing HA-tagged CFTR-ΔF508. Fold change of band C not shown, as no band C detected in Scr and UnT samples. (*C*) Anti-HA antibody (Covance). (*D*) Anti-CFTR antibody (R769 antibody). Based on results in HeLa cells (Fig. 2E, SI Fig. S5) and the increase in endogenous *CFTR* mRNA (SI Fig. S9B) in response to miR-138 mimic or SIN3A DsiRNA, the increased abundance of CFTR band C represents the sum of both the increased abundance of HA-tagged CFTR-ΔF508 processing as well as endogenous CFTR protein expression. Error bars indicate mean ± SE; **P* <0.01 relative to Scr; $^{\#}P$ <0.01, relative to Scr CFTR band B.

Fig. S10A.

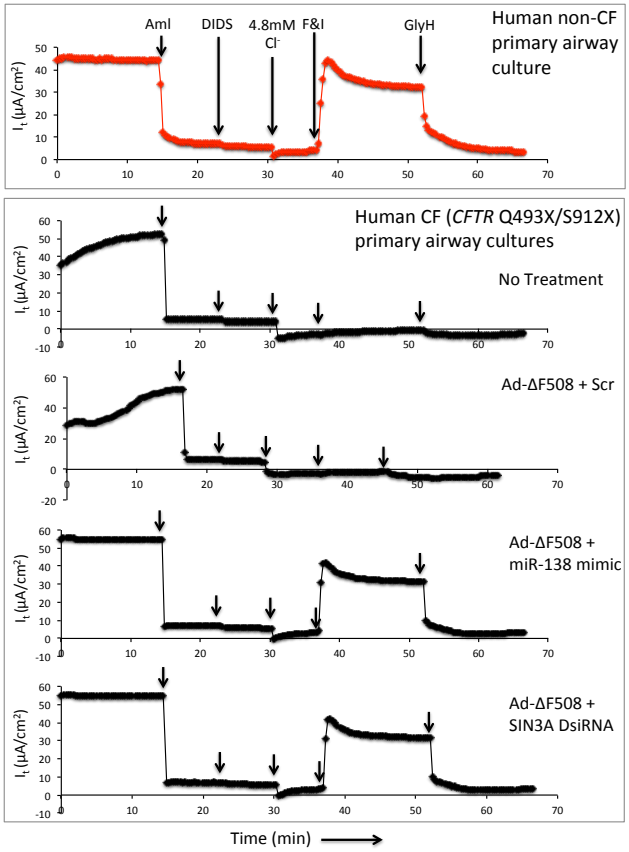

Fig. S10B.

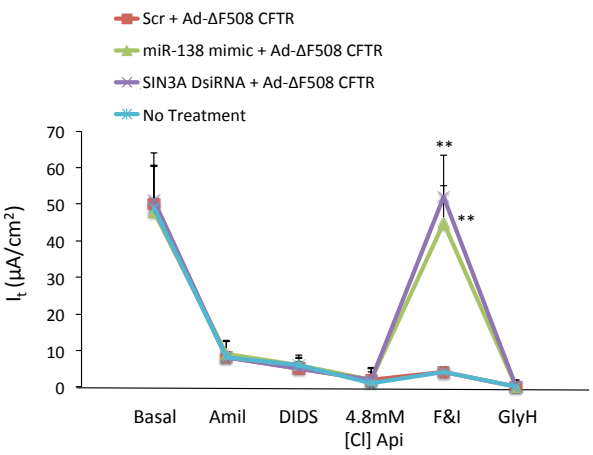

Fig. S11.

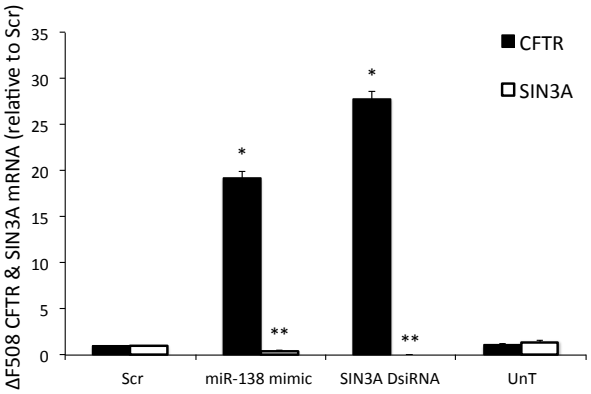

Fig. S10. SIN3A inhibition yields partial rescue of Cl^- transport in CF epithelia. (*A*) Representative tracings of transepithelial current (I_t) responses after sequential apical application of noted reagents in primary *CFTR* null human airway epithelial (*CFTR* Q493X/S912X). (*B*) Average transepithelial current (I_t) responses after sequential apical application of noted reagents in primary airway epithelia (*CFTR* Q493X/S912X). Aml=Amiloride. Each data point represented by 3 cultures. Basal transepithelial resistance range: 279-360 ohms*cm^2. Error bars indicate mean ± SE, **P* <0.01, relative to Scr (SIN3A); ***P* <0.01, relative to Scr after F&I stimulation.

Fig. S11. miR-138 regulates endogenous CFTR and SIN3A expression in CF primary airway epithelia. Relative *CFTR*-ΔF508 and *SIN3A* mRNA abundance in 4 human donors of CF (ΔF508/ΔF508) primary airway epithelia 24 hrs post-transfection (8 replicates per donor). Error bars indicate mean ± SE, **P* <0.01, relative to Scr (for CFTR); ***P* <0.01, relative to Scr (for SIN3A).

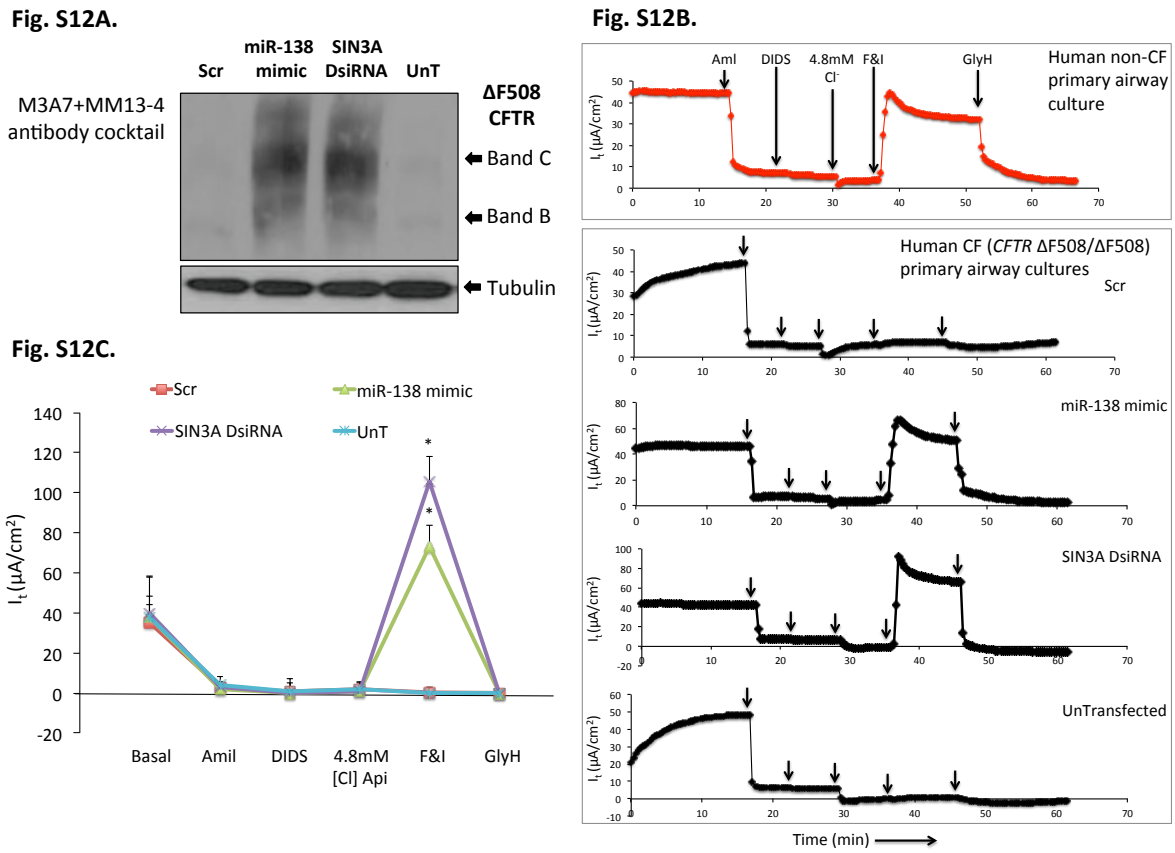

Fig. S12. SIN3A inhibition yields partial rescue of Cl^- transport in CF epithelia. (*A*) CFTR-ΔF508 immunoblot in a human donor of primary CF (ΔF508/ΔF508) primary airway epithelia 72 hrs post-transfection (8 replicates, Donor #2 on Fig. 4D; M3A7+MM13-4 antibody cocktail). (*B*) Representative tracings of transepithelial current (I_t) response after sequential apical application of noted reagents in primary airway epithelia (*CFTR* ΔF508/ΔF508). (*C*) Average transepithelial current (I_t) responses after sequential apical application of noted reagents. Each data point represented by 8 cultures. Basal transepithelial resistance range: 488-691 ohms*cm^2. Error bars indicate mean ± SE, **P* <0.01 relative to Scr after F&I stimulation.

Fig. S13A.

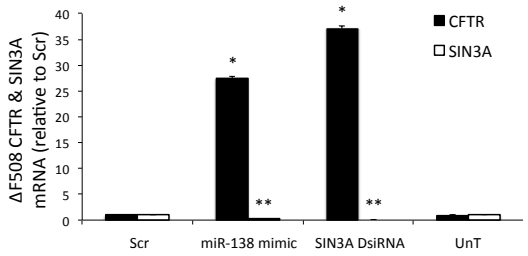

Fig. S13B.

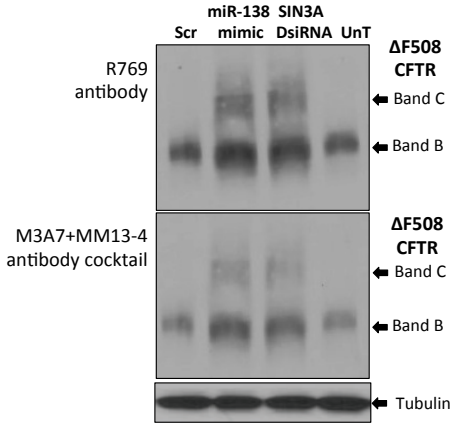

Fig. S13C.

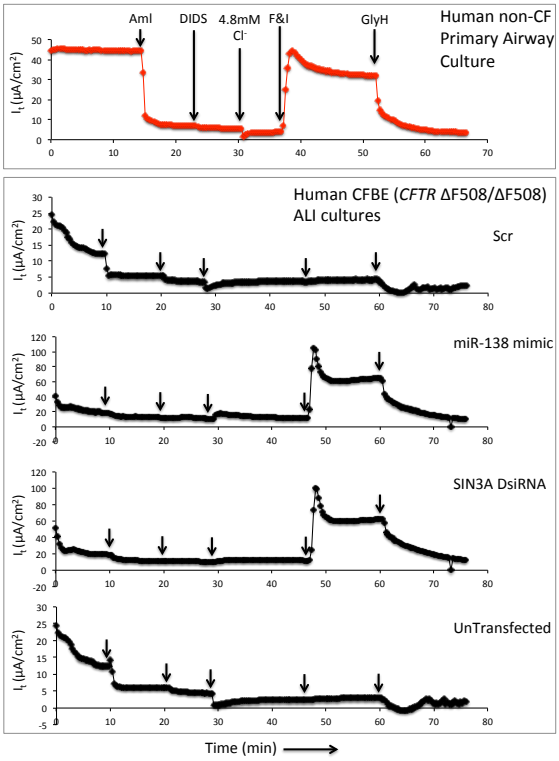

Fig. S13D.

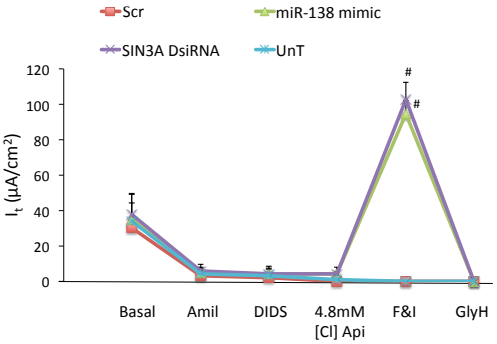

Fig. S13E.

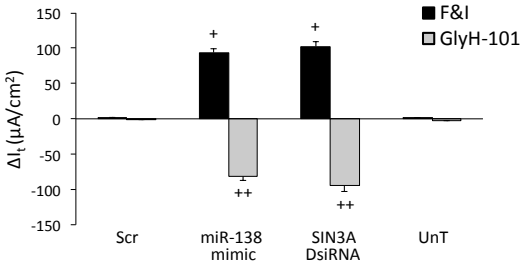

Fig. S13. miR-138 regulates endogenous CFTR and SIN3A expression in CFBE cells. (*A*) Relative *CFTR*-ΔF508 and *SIN3A* mRNA abundance in CFBE cells (*CFTR* ΔF508/ΔF508) 24 hrs post-transfection (n=4, 8 replicates). (*B*) Representative CFTR immunoblot in CFBE cells performed 72 hrs post-transfection (n=4, 8 replicates). PVDF membrane was first probed with R769 antibody (top panel), stripped and re-probed with the M3A7+MM13-4 antibody cocktail (bottom panel). (*C*) Representative tracings of transepithelial current (I_t) response after sequential apical application of noted reagents in CFBE cells (*CFTR* ΔF508/ΔF508). (*D*) Average transepithelial current (I_t) responses after sequential apical application of noted reagents. Each data point represented by 8 CFBE ALI cultures. Basal transepithelial resistance range: 478-611 ohms*cm^2. (*E*) Change in transepithelial current (ΔI_t) after stimulation with Forskolin + IBMX (F&I) and GlyH. Each data point represented by 8 CFBE ALI cultures. All panels, Error bars indicate mean ± SE. **P* <0.01, relative to Scr (CFTR); ***P* <0.01, relative to Scr (SIN3A); $^{\#}P$ <0.01 relative to I_t in Scr transfected samples upon F&I addition; ^{+}P <0.01 and ^{++}P <0.01 relative to ΔI_t in Scr transfected samples upon F&I or GlyH-101 stimulation respectively.

Fig. S14A.

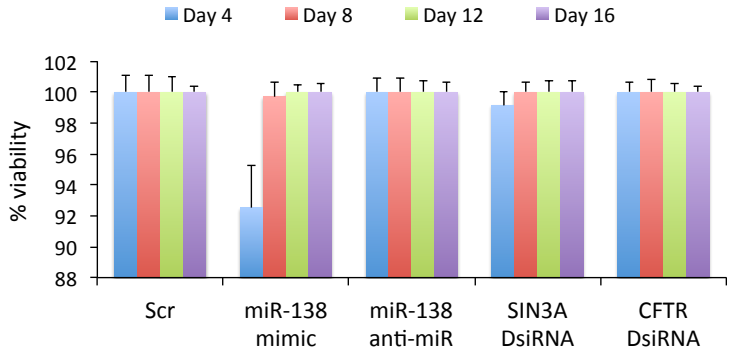

Fig. S14B.

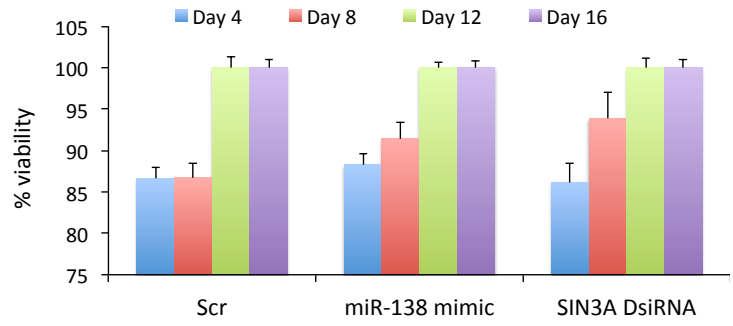

Fig. S14. Oligonucleotide transfection does not cause decrease in cell viability. Percentage viability calculated in (*A*) Calu-3 cells and (*B*) CFBE cells as a measure of lactate dehydrogenase release 4, 8, 12, and 16 days post-transfection with noted oligonucleotides. Measurements were normalized to untransfected cells. Each bar represents three independent experiments

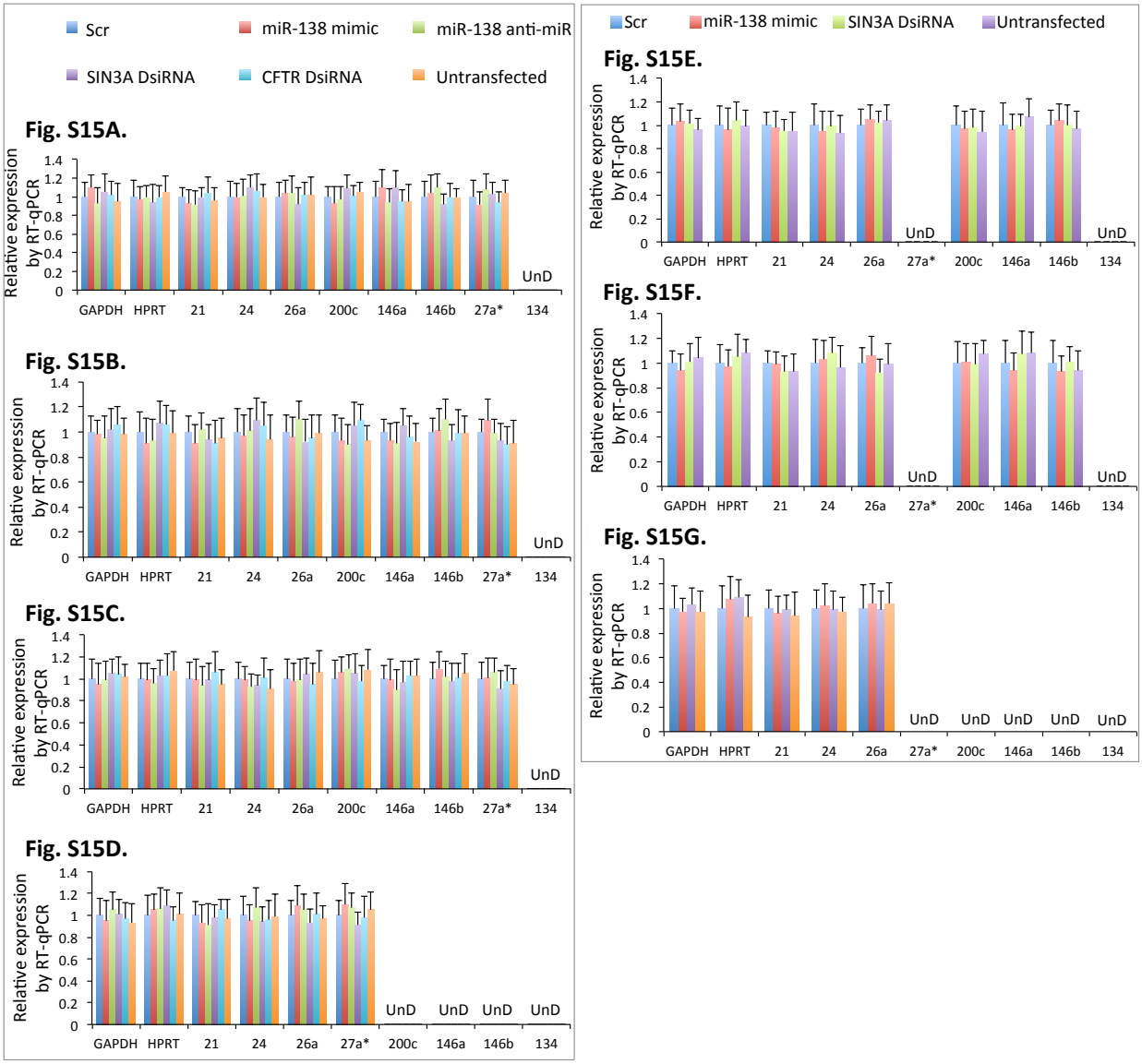

Fig. S15. Specificity of oligonucleotide transfections. Relative expression by RT-qPCR of GAPDH and HPRT (normalized to SFRS9), and miRs -21, -24, -26a, -200c, -146a, -146b, -27a*, -134 (normalized to RNU48). Experiment performed 24 hrs post-transfection in (*A*) Primary airway epithelia from human non-CF donor #1 (6 replicates), (*B*) Primary airway epithelia from human non-CF donor #2 (6 replicates), (*C*) Primary airway epithelia from human non-CF donor #3 (6 replicates), (*D*) Calu-3 cells (n=4, 6 replicates each), (*E*) HEK293T cells (n=4, 6 replicates each), (*F*) HeLa cells (n=4, 6 replicates each), and (*G*) CFBE (*CFTR* ΔF508/ΔF508) cells (n=4, 6 replicates each). All panels, Error bars indicate mean ± SE. UnD= Undetected by RT-qPCR.

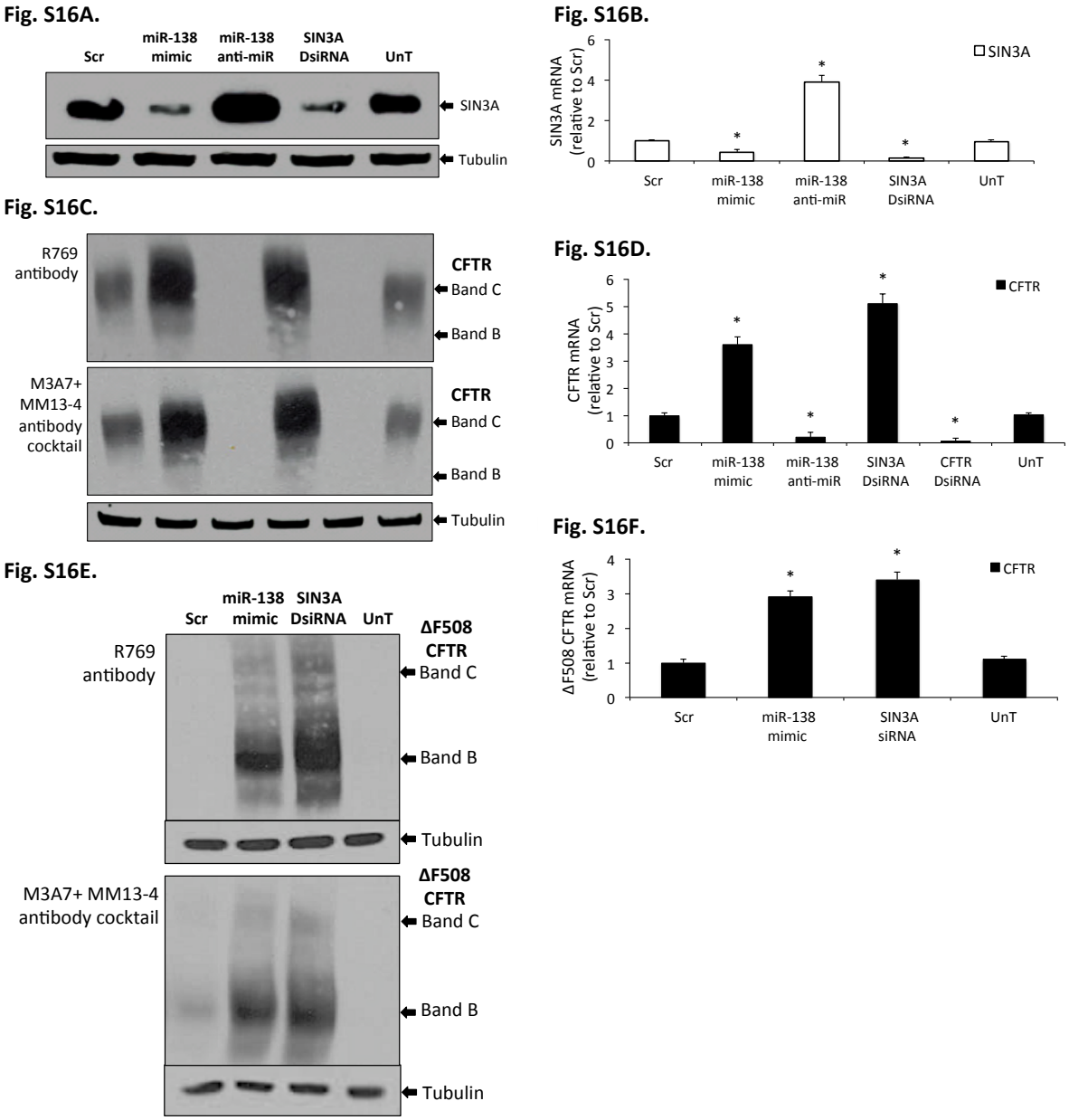

Fig. S16. Persistence of oligonucleotide effects 2 weeks post-transfection. (*A*) Representative SIN3A immunoblot in Calu-3 air-liquid interface (ALI) cultures 14 days post-transfection (6 replicates). (*B*) Relative SIN3A mRNA abundance in Calu-3 ALI cultures 14 days post transfection (6 replicates). (*C*) Representative CFTR immunoblot in Calu-3 ALI cultures 14 days post-transfection (8 replicates). PVDF membrane was first probed with R769 antibody (top panel), stripped and re-probed with the M3A7+MM13-4 antibody cocktail (bottom panel). (*D*) Relative *CFTR* mRNA abundance in Calu-3 ALI cultures 14 days post transfection (6 replicates). (*E*) Representative CFTR immunoblot in CFBE (*CFTR* ΔF508/ΔF508) ALI cultures 14 days post-transfection (6 replicates) (top panel-R769 antibody, bottom panel-M3A7+MM13-4 antibody cocktail). (*F*) Relative *CFTR* mRNA abundance in CFBE ALI cultures 14 days post-transfection (6 replicates). All panels, Error bars indicate mean ± SE. **P* <0.01, relative to Scr.

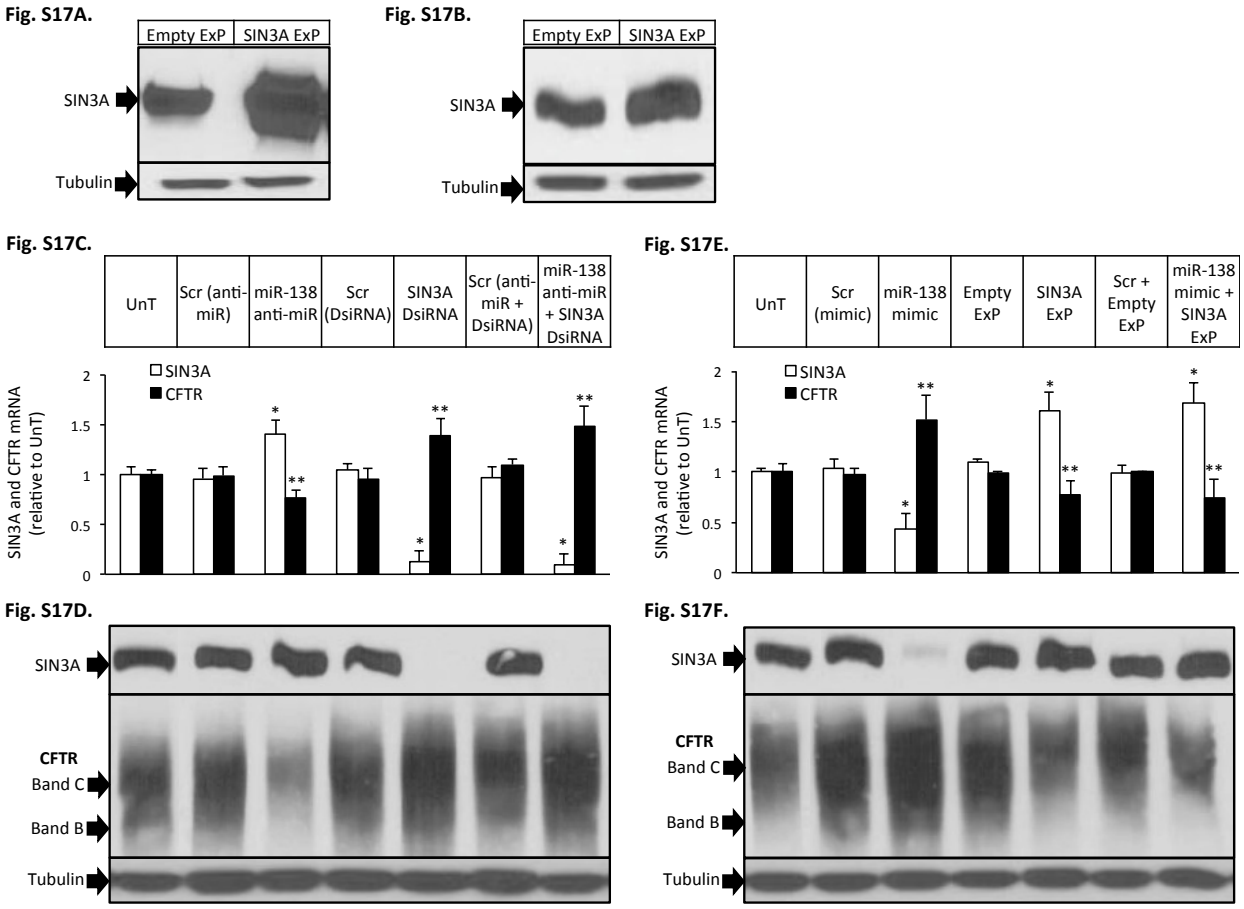

Fig. S17. Epistatic relationship between SIN3A and miR-138. (*A*) SIN3A expression in HEK293T cells assessed by western blot 48 hrs post transfection with empty vector (Empty ExP) or SIN3A cDNA (SIN3A ExP). (*B*) SIN3A expression in Calu-3 cells assessed by western blot 48 hrs post transfection with empty vector or SIN3A cDNA. (*C* and *E*) Relative *SIN3A* and *CFTR* mRNA levels in Calu-3 cells 48 hrs post transfection (3 replicates). (*D* and *F*) Representative SIN3A and CFTR immunoblots in Calu-3 cells 48 hrs post transfection (3 replicates). All panels, Error bars indicate mean ± SE. **P* <0.05, relative to UnT (SIN3A); ***P* <0.05, relative to UnT (CFTR). ExP denotes expression plasmid.

Table S1. Expression of microRNAs in human airway epithelia

AB TaqMan® Low Density MicroRNA Array (TLDA) was performed on 4 human non-CF primary well-differentiated airway epithelial cultures. With a C_q cut-off <30, 115 miRNAs were deemed expressed in the human airway epithelium. Of these, 31 miRNAs (**bold**) were highly expressed with an average $C_q$value <25. MiRNAs arranged in order of their decreasing average abundance.

microRNA-(probeset ID)	Cq (Donor#1)	Cq (Donor#2)	Cq (Donor#3)	Cq (Donor#4)
hsa-miR-30a*-4373062	**24.6**	**24.2**	**24.2**	**24.4**
hsa-miR-186-4395396	**24.0**	**23.6**	**24.0**	**23.9**
hsa-miR-24-4373072	**21.2**	**20.8**	**21.2**	**20.8**
hsa-miR-200c-4395411	**21.2**	**20.9**	**20.8**	**21.3**
hsa-miR-484-4381032	**23.7**	**23.3**	**24.0**	**23.9**
hsa-miR-191-4395410	**22.0**	**21.4**	**21.5**	**21.5**
hsa-miR-16-4373121	**22.0**	**22.1**	**22.6**	**22.0**
hsa-miR-30e-4395334	**23.2**	**23.1**	**23.7**	**23.7**
hsa-miR-17-4395419	**24.3**	**23.5**	**23.8**	**23.9**
hsa-miR-106a-4395280	**24.1**	**23.2**	**23.7**	**23.8**
hsa-miR-378-4395354	**24.6**	**23.8**	**24.4**	**24.6**
hsa-miR-138-4395395	**24.0**	**24.4**	**23.6**	**23.5**
hsa-miR-19b-4373098	**23.2**	**22.4**	**22.4**	**23.1**
hsa-miR-31-4395390	**23.0**	**22.1**	**22.8**	**21.9**
hsa-miR-30c-4373060	**23.0**	**22.2**	**22.0**	**23.1**
hsa-miR-200a-4378069	**24.1**	**23.3**	**23.0**	**24.1**
hsa-miR-222-4395387	**19.7**	**19.6**	**20.5**	**20.8**
hsa-miR-768-3p-4395188	**24.0**	**24.3**	**24.8**	**25.5**
hsa-miR-768-3p-4395188	**24.0**	**24.0**	**24.6**	**25.4**
hsa-miR-203-4373095	**25.0**	**24.7**	**23.8**	**23.6**
hsa-miR-29a-4395223	**22.2**	**21.7**	**21.8**	**23.2**
hsa-miR-200b-4395362	**22.6**	**21.6**	**21.0**	**22.5**
hsa-miR-141-4373137	**24.4**	**23.4**	**23.2**	**24.8**
hsa-miR-30b-4373290	**23.5**	**22.7**	**22.0**	**23.7**
hsa-miR-26b-4395167	**25.6**	**24.4**	**24.1**	**25.7**
hsa-miR-26a-4395166	**24.7**	**23.1**	**22.8**	**24.5**
hsa-miR-21-4373090	**24.2**	**22.6**	**22.7**	**24.4**
hsa-miR-429-4373203	**25.7**	**23.8**	**23.5**	**24.8**
hsa-miR-449a-4373207	**23.3**	**21.9**	**22.6**	**21.0**
hsa-miR-146a-4373132	**22.7**	**21.8**	**26.9**	**23.5**
hsa-miR-574-3p-4395460	25.4	24.9	25.0	25.1
hsa-miR-125a-5p-4395309	24.9	25.1	25.2	25.5

hsa-miR-151-3p-4395365	25.5	25.1	25.4	25.2
hsa-miR-223-4395406	26.3	24.9	26.1	24.5
hsa-let-7g-4395393	26.1	25.2	24.5	25.9
hsa-let-7e-4395517	26.6	25.6	24.0	25.9
hsa-miR-30a-4373061	25.8	25.1	25.5	26.0
hsa-miR-135b-4395372	26.5	25.5	25.5	25.0
hsa-miR-135a*-4395343	25.5	25.8	25.5	26.0
hsa-miR-342-3p-4395371	26.2	25.3	25.7	25.8
hsa-miR-27a-4373287	26.8	25.3	25.3	25.9
hsa-miR-454-4395434	26.2	25.4	25.8	25.9
hsa-miR-19a-4373099	26.3	25.2	25.8	26.4
hsa-miR-34c-5p-4373036	27.7	25.1	23.8	27.1
hsa-miR-320-4395388	25.8	26.1	26.2	25.9
hsa-miR-449b-4381011	27.7	25.9	25.6	24.8
hsa-miR-29c-4395171	26.2	25.5	25.6	27.0
hsa-miR-20a-4373286	27.3	25.6	25.1	26.8
hsa-miR-345-4395297	26.7	26.3	25.7	26.1
hsa-miR-374b-4381045	26.8	26.0	25.5	26.5
hsa-miR-149-4395366	27.3	27.4	25.1	25.5
hsa-miR-331-3p-4373046	26.9	26.2	26.2	26.3
hsa-miR-93-4373302	27.9	26.1	25.7	26.8
hsa-miR-132-4373143	26.7	26.1	26.5	27.3
hsa-miR-140-5p-4373374	26.8	26.0	26.4	27.5
hsa-miR-28-3p-4395557	26.8	26.7	26.5	26.8
hsa-miR-93*-4395250	27.1	26.8	27.0	26.1
hsa-miR-146b-5p-4373178	26.6	26.4	27.3	27.1
hsa-miR-34a-4395168	27.6	26.5	25.7	27.7
hsa-miR-590-5p-4395176	27.2	26.5	26.9	27.3
hsa-miR-30d-4373059	27.3	26.4	26.9	27.8
hsa-miR-532-5p-4380928	28.0	26.6	26.8	27.2
hsa-miR-30d-4373059	27.4	26.5	27.0	27.8
hsa-miR-374a-4373028	28.0	26.9	26.6	27.5
hsa-miR-34b*-4373037	27.7	26.4	26.1	29.2
hsa-miR-422a-4395408	27.7	26.7	27.3	27.6
hsa-miR-125b-4373148	28.5	26.9	25.5	28.5
hsa-miR-708-4395452	28.2	26.7	27.3	27.3
hsa-miR-801-4395183	27.6	27.4	27.2	27.6
hsa-miR-801-4395183	27.5	27.4	27.4	27.9
hsa-miR-106b-4373155	28.6	27.4	26.7	27.6
hsa-miR-660-4380925	28.3	27.0	27.2	28.0
hsa-miR-99a-4373008	29.1	27.4	25.9	28.3
hsa-miR-150-4373127	27.5	27.1	26.6	29.4
hsa-miR-100-4373160	29.0	27.8	26.0	28.2

hsa-miR-7-1*-4381118	27.4	27.9	27.8	28.1
hsa-miR-205-4373093	29.8	27.8	26.5	27.3
hsa-miR-200a*-4373273	27.7	27.8	28.1	27.8
hsa-miR-224-4395210	28.7	27.0	27.9	28.0
hsa-miR-195-4373105	28.5	27.5	27.8	28.1
hsa-miR-425-4380926	28.9	27.9	27.6	28.1
hsa-miR-625*-4395543	27.5	28.1	28.2	28.6
hsa-miR-27b-4373068	29.2	27.8	27.1	28.6
hsa-miR-152-4395170	29.1	27.6	27.2	29.1
hsa-miR-218-4373081	28.7	26.8	28.7	28.9
hsa-let-7b-4395446	29.8	28.5	26.2	28.7
hsa-miR-148a-4373130	29.5	28.1	27.2	28.7
hsa-miR-182-4395445	28.7	29.0	28.2	28.1
hsa-miR-210-4373089	29.2	28.4	28.2	28.4
hsa-miR-628-5p-4395544	28.6	28.2	28.4	29.2
hsa-miR-103-4373158	29.9	28.4	27.3	28.8
hsa-miR-92a-4395169	29.5	28.9	27.7	28.8
hsa-miR-15b-4373122	30.1	28.7	27.3	29.0
hsa-miR-34a*-4395427	28.3	29.1	29.0	29.0
hsa-miR-375-4373027	30.1	28.5	27.6	29.2
hsa-miR-221-4373077	30.5	28.5	27.3	29.4
hsa-miR-340-4395369	30.1	28.2	27.8	29.6
hsa-miR-192-4373108	28.9	28.5	29.3	29.3
hsa-miR-452-4395440	29.2	29.1	29.0	28.7
hsa-let-7a-4373169	30.5	28.9	27.1	29.8
hsa-miR-25-4373071	29.5	29.1	28.5	29.2
hsa-miR-598-4395179	30.0	28.9	28.1	29.9
hsa-miR-886-3p-4395305	28.1	28.7	29.6	30.4
hsa-miR-744-4395435	30.3	29.0	28.2	29.3
hsa-miR-126-4395339	29.3	29.7	29.6	28.4
hsa-let-7d-4395394	30.2	29.4	27.6	29.8
hsa-miR-532-3p-4395466	29.9	28.7	28.4	30.0
hsa-miR-28-5p-4373067	30.0	29.0	28.4	29.8
hsa-miR-339-3p-4395295	29.0	29.0	29.8	29.7
hsa-miR-193b-4395478	29.0	31.5	29.7	27.6
hsa-miR-99b-4373007	30.1	29.7	28.4	29.8
hsa-miR-200b*-4395385	30.2	29.8	28.8	29.7
hsa-miR-491-5p-4381053	30.9	29.6	29.5	29.6
hsa-miR-188-5p-4395431	29.6	30.0	30.1	30.1

Table S2. CFTR-Associated Gene Network (16, 25-28)

This gene list was curated from the published literature (16, 25-28) and includes gene products as identified as directly or indirectly involved in CFTR biosynthesis.

Gene Symbol	Description	Gene Symbol	Description
MARCH2	membrane-associated ring finger (C3HC4) 2	LMO7	LIM domain 7
MARCH3	membrane-associated ring finger (C3HC4) 3	LRRFIP2	leucine rich repeat (in FLII) interacting protein 2
MARCH5	membrane-associated ring finger (C3HC4) 5	MARCKSL 1	MARCKS-like 1
SEPT1	Septin-1	MDM2	Mdm2 p53 binding protein homolog (mouse)
SEPT2	Septin-2	MLP	membrane lipoprotein precursor
SEPT3	Septin-3	MMS19	MMS19 nucleotide excision repair homolog (S. cerevisiae)
SEPT6	Septin-6	MMS19L	MMS19-like (MET18 homolog, S. cerevisiae)
A2M	alpha-2-macroglobulin homologue	MS4A5	membrane-spanning 4-domains, subfamily A, member 5
ADCY8	adenylate cyclase 8 (brain)	MTAP4	microtubule-associated protein 4
AHA1	Hsp90 co-chaperone AHA1	MUC13	mucin 13, cell surface associated
AHSA1	AHA1, activator of heat shock protein ATPase homolog 1 (yeast)	MUC2	mucin 2, oligomeric mucus/gel-forming
AHSA2	AHA1, activator of heat shock 90kDa protein ATPase homolog 2 (yeast)	NEDD4	similar to E3 ubiquitin-protein ligase Nedd-4
AIFM1	apoptosis-inducing factor, mitochondrion-associated, 1	NEDD4L	Nedd4 protein
AKAP6	A kinase (PRKA) anchor protein 6	NKX2-1	NK2 homeobox 1
AMFR	similar to autocrine motility factor receptor; autocrine motility factor receptor	NPEPPS	aminopeptidase puromycin sensitive
ANO1	anoctamin 1, calcium activated chloride channel	NRIP3	nuclear receptor interacting protein 3
AP1B1	adaptor protein complex AP-1, beta 1 subunit	NUAK1	NUAK family, SNF1-like kinase, 1
APC	adenomatous polyposis coli	OPRS1	opioid receptor, sigma 1
APOA2	apolipoprotein A-II	P4HA1	prolyl 4-hydroxylase, alpha polypeptide I
AQP1	aquaporin 1 (Colton blood	PACRG	PARK2 co-regulated

	group)		
ARF4	ADP-ribosylation factor 4	PARC	DNA topoisomerase 4 subunit A
ARIH1	ariadne homolog, ubiquitin-conjugating enzyme E2 binding protein, 1 (Drosophila)	PARK10	Parkinson disease 10
ATAD3A	ATPase family, AAA domain containing 3A	PARK12	Parkinson disease (X-linked) 12
ATP2A1	ATPase, Ca++ transporting, cardiac muscle, slow twitch 2	PARK2	Parkinson disease (autosomal recessive, juvenile) 2, parkin
ATP2A2	ATPase, Ca++ transporting, cardiac muscle, slow twitch 2	PARK3	Parkinson disease (autosomal dominant, Lewy body) 3
ATP2A3	ATPase, Ca++ transporting, ubiquitous	PARK4	Parkinson disease (autosomal dominant, Lewy body) 4
ATP6V1A	ATPase, H+ transporting, lysosomal 70kDa, V1 subunit A	PARK7	Parkinson disease (autosomal recessive, early onset) 7
ATXN2L	ataxin 2-like	PCDH15	protocadherin 15
B3GNT9	UDP-GlcNAc:betaGal beta-1,3-N-acetylglucosaminyltransferase 9	PCDHB8	protocadherin beta 8
BAG1	BCL2-associated athanogene	PCMT1	protein-L-isoaspartate (D-aspartate) O-methyltransferase 1
BAG2	BCL2-associated athanogene 2	PDCD6	aryl-hydrocarbon receptor repressor; programmed cell death 6
BAG3	BCL2-associated athanogene 3	PDCD8	programmed cell death 8 (apoptosis-inducing factor)
BCR	breakpoint cluster region	PDDC1	Parkinson disease 7 domain containing 1
BIRC6	baculoviral IAP repeat-containing 6	PDE8A	phosphodiesterase 8A
C6orf48	chromosome 6 open reading frame 48; small nucleolar RNA, C/D box 52	PDZK1	PDZ domain containing 1
C8orf55	chromosome 8 open reading frame 55	PHLDB3	pleckstrin homology-like domain, family B, member 3
C9ORF10	similar to Family with sequence similarity 120A	PKC	protein kinase C
CAL	Transcription factor CAULIFLOWER	PKD1	polycystic kidney disease 1 homolog (human)
CALU	calumenin	PLD	phospholipase D1, phosphatidylcholine-specific
CANX	calnexin	PLD2	phospholipase D2
CAPNS1	calpain, small subunit 1	PLEKHA6	pleckstrin homology domain containing, family A member 6
CAPRIN1	cell cycle associated protein 1	PPIB	peptidylprolyl isomerase B (cyclophilin B)
CBL	Cas-Br-M (murine) ecotropic retroviral transforming sequence	PPID	peptidylprolyl isomerase D

CCT1	T-complex protein 1, alpha subunit	PPIL2	peptidylprolyl isomerase (cyclophilin)-like 2
CCT3	chaperonin containing TCP1, subunit 3 (gamma)	PPP2CA	protein phosphatase 2 (formerly 2A), catalytic subunit, alpha isoform
CCT4	chaperonin containing Tcp1, subunit 4 (delta)	PPP2CB	protein phosphatase 2 (formerly 2A), catalytic subunit, beta isoform
CCT5	chaperonin containing TCP1, subunit 5 (epsilon)	PPP2R1A	protein phosphatase 2, regulatory subunit A, alpha isoform
CD36	CD36 molecule (thrombospondin receptor)	PPP2R1B	protein phosphatase 2 (formerly 2A), regulatory subunit A, beta isoform
CD46	CD46 molecule, complement regulatory protein	PPP2R2A	protein phosphatase 2, regulatory subunit B, alpha
CD59	CD59 molecule, complement regulatory protein	PPP2R2B	protein phosphatase 2 (formerly 2A), regulatory subunit B, beta isoform
CDC37	cell division cycle 37 homolog (S. cerevisiae)	PRG4	proteoglycan 4
CDH1	cadherin 1	PRKAA1	protein kinase, AMP-activated, alpha 1 catalytic subunit
CDK5R1	cyclin-dependent kinase 5, regulatory subunit 1 (p35)	PRKAA2	protein kinase, AMP-activated, alpha 2 catalytic subunit
CEP170	centrosomal protein 170kDa	PRKAB1	protein kinase, AMP-activated, beta 1 non-catalytic subunit
CFL1	cofilin 1 (non-muscle)	PRKAB2	protein kinase, AMP-activated, beta 2 non-catalytic subunit
CFTR	**cystic fibrosis transmembrane conductance regulator, ATP-binding cassette (sub-family C, member 7)**	PRKAG1	protein kinase, AMP-activated, gamma 1 non-catalytic subunit
CLCA1	chloride channel accessory 1	PRKAG2	protein kinase, AMP-activated, gamma 2 non-catalytic subunit
CLINT1	hypothetical protein MGC97891	PRKAG3	protein kinase, AMP-activated, gamma 3 non-catatlytic subunit
CLN2	G1/S-specific cyclin CLN2	PRKAR2A	protein kinase, cAMP-dependent, regulatory, type II, alpha
CLTA	clathrin, light chain (Lca)	PRKDC	protein kinase, DNA-activated, catalytic polypeptide
CLTCL1	clathrin, heavy chain-like 1	PRP19	PRP19/PSO4 pre-mRNA processing factor 19 homolog (S. cerevisiae)
COPB	coatomer protein complex, subunit beta	PSAP	prosaposin
COPB1	coatomer protein complex, subunit beta 1	PSENEN	presenilin enhancer 2 homolog (C. elegans)
COPB2	coatomer protein complex, subunit beta 2	PSMA1	proteasome (prosome, macropain) subunit, alpha type, 1
CSE1L	CSE1 chromosome segregation 1-like (yeast)	PSMA2	proteasome (prosome, macropain) subunit, alpha type, 2

CSRP3	cysteine and glycine-rich protein 3 (cardiac LIM protein)	PSMB1	proteasome (prosome, macropain) subunit, beta type, 1
CSTB	cystatin B (stefin B)	PSMB3	proteasome (prosome, macropain) subunit, beta type, 3;
CUL7	cullin 7	PSMB4	proteasome (prosome, macropain) subunit, beta type, 4
CYB5B	cytochrome b5 type B (outer mitochondrial membrane)	PSMC3IP	PSMC3 interacting protein
CYPB	Peptidyl-prolyl cis-trans isomerase	PSMC4	proteasome (prosome, macropain) 26S subunit, ATPase, 4
DAB2	disabled homolog 2, mitogen-responsive phosphoprotein (Drosophila)	PSMD11	proteasome (prosome, macropain) 26S subunit, non-ATPase, 11
DCLK1	doublecortin-like kinase 1	PSMD2	proteasome (prosome, macropain) 26S subunit, non-ATPase, 2
DERL1	Der1-like domain family, member 1	PSME2	proteasome (prosome, macropain) activator subunit 2 (PA28 beta)
DNAJA1	DnaJ (Hsp40) homolog, subfamily A, member 1	PTGES3	unactive progesterone receptor, 23 kD
DNAJA2	DnaJ (Hsp40) homolog, subfamily A, member 2	PTPRC	protein tyrosine phosphatase, receptor type, C
DNAJA3	DnaJ (Hsp40) homolog, subfamily A, member 3	RAN	RAN, member RAS oncogene family
DNAJB1	DnaJ (Hsp40) homolog, subfamily B, member 1	RANBP1	similar to RAN binding protein 1; RAN binding protein 1
DNAJB12	DnaJ (Hsp40) homolog, subfamily B, member 12	RCN1	reticulocalbin 1, EF-hand calcium binding domain
DNAJB2	DnaJ (Hsp40) homolog, subfamily B, member 2	RCN2	Regulator of calcineurin 2
DNAJB4	DnaJ (Hsp40) homolog, subfamily B, member 4	REPS1	RALBP1 associated Eps domain containing 1
DNAJB5	DnaJ (Hsp40) homolog, subfamily B, member 5	RGAG4	retrotransposon gag domain containing 4
DNAJC27	DnaJ (Hsp40) homolog, subfamily C, member 27	RHOJ	ras homolog gene family, member J
DNAJC3	DnaJ (Hsp40) homolog, subfamily C, member 3	RHOQ	ras homolog gene family, member Q
DNAJC5	DnaJ (Hsp40) homolog, subfamily C, member 5	RHOT1	ras homolog gene family, member T1
DNAJC7	DnaJ (Hsp40) homolog, subfamily C, member 7	RMA1	Probable folylpolyglutamate synthase
DNCH1	dynein, cytoplasmic, heavy polypeptide 1	RNF128	ring finger protein 128
DPYSL2	dihydropyrimidinase-like 2	RNF5	ring finger protein 5
DTL	denticleless homolog	RPS27A	ribosomal protein S27a

	(Drosophila)		
DYNC1H1	dynein, cytoplasmic 1, heavy chain 1	RRAS	related RAS viral (r-ras) oncogene homolog
EDG4	endothelial differentiation, lysophosphatidic acid G-protein-coupled receptor, 4	RS1	retinoschisin 1
EFHA1	EF-hand domain family, member A1	RSC1A1	regulatory solute carrier protein, family 1, member 1
EMD	emerin	RTL1	rettrotransposon-like 1
ENTHD1	ENTH domain containing 1	RUVBL1	RuvB-like 1 (E. coli)
EPS8	epidermal growth factor receptor pathway substrate 8	RUVBL2	RuvB-like 2 (E. coli)
ERBB2	v-erb-b2 erythroblastic leukemia viral oncogene homolog 2	RYK	receptor-like tyrosine kinase
EXO1	Exodeoxyribonuclease 1	RYR2	ryanodine receptor 2, cardiac
FAM120A	Constitutive coactivator of PPAR-gamma-like protein 1	RYR3	ryanodine receptor 3
FAM83A	family with sequence similarity 83, member A	S100A6	S100 calcium binding protein A6
FARSA	phenylalanyl-tRNA synthetase, alpha subunit	S100A7	S100 calcium binding protein A7
FARSB	phenylalanyl-tRNA synthetase, beta subunit	S100A9	S100 calcium binding protein A9
FAT1	FAT tumor suppressor homolog 1 (Drosophila)	SAFB	scaffold attachment factor B
FAT2	FAT tumor suppressor homolog 2 (Drosophila)	SAR1B	SAR1 homolog B (S. cerevisiae)
FCNA	ficolin A	SEC31A	SEC31 homolog A (S. cerevisiae)
FKBP8	FK506 binding protein 8, 38kDa	SEC61A1	Sec61 alpha 1 subunit (S. cerevisiae)
FLOT2	flotillin 2	SEC61A2	dehydrogenase E1 and transketolase domain containing 1; Sec61 alpha 2 subunit (S. cerevisiae)
FN1	fibronectin 1	SERP1	stress-associated endoplasmic reticulum protein 1
GNA11	guanine nucleotide binding protein (G protein), alpha 11 (Gq class)	SFXN3	sideroflexin 3
GNAI2	guanine nucleotide binding protein (G protein), alpha inhibiting activity polypeptide 2	SH3BGRL 2	SH3 domain binding glutamic acid-rich protein like 2
GNB2L1	guanine nucleotide binding protein (G protein), beta polypeptide 2-like 1	SHROOM3	shroom family member 3
GOPC	golgi associated PDZ and coiled-coil motif containing	SIAH1	seven in absentia homolog 1 (Drosophila)

GRIP1	glutamate receptor interacting protein 1	**SIN3A**	**SIN3 homolog A, transcription regulator (yeast)**
GRN	granulin	SLC9A2	solute carrier family 9 (sodium/hydrogen exchanger), member 2
GRP78	glucose-regulated protein 78kDa	SLC9A3R1	similar to solute carrier family 9 (sodium/hydrogen exchanger), isoform 3 regulator 1
GUCY2D	guanylate cyclase 2D, membrane (retina-specific)	SLC9A3R2	solute carrier family 9 (sodium/hydrogen exchanger), member 3 regulator 2
HACE1	HECT domain and ankyrin repeat containing, E3 ubiquitin protein ligase 1	SMURF1	SMAD specific E3 ubiquitin protein ligase 1
HAX1	HCLS1 associated X-1; silica-induced gene 111	SNX26	sorting nexin 26
HCLS1	hematopoietic cell specific Lyn substrate 1	SNX4	sorting nexin 4
HOP	Halorhodopsin	SNX9	sorting nexin 9
HOPX	odd homeobox 1 protein	SOD2	Superoxide dismutase [Mn], mitochondrial
HSC70	heat shock protein 70 cognate	SORL1	sortilin-related receptor, LDLR class A repeats-containing
HSD3B1	hydroxy-delta-5-steroid dehydrogenase, 3 beta- and steroid delta-isomerase 1	SPTLC1	serine palmitoyltransferase, long chain base subunit 1
HSP22	Heat shock protein 22; Heat shock gene 67Bb	SQRDL	sulfide quinone reductase-like (yeast)
HSP25	heat shock protein 25	SRA1	steroid receptor RNA activator 1
HSP27	Heat shock protein 27	ST13	suppression of tumorigenicity 13 (colon carcinoma) (Hsp70 interacting protein)
HSP47	heat shock protein 47	STAM2	signal transducing adaptor molecule (SH3 domain and ITAM motif) 2
HSP60	Heat shock protein 60, mitochondrial	STIP1	stress-induced-phosphoprotein 1
HSPA1A	heat shock 70kDa protein 1A	STUB1	STIP1 homology and U-box containing protein 1
HSP90AA1	heat shock protein 90, alpha (cytosolic), class A member 1	STX1A	syntaxin 1A (brain)
HSP90AA2	heat shock protein 90kDa alpha (cytosolic), class A member 2; heat shock protein 90kDa alpha (cytosolic), class A member 1	SVIL	supervillin
HSP90AA4P	heat shock protein 90kDa alpha (cytosolic), class A member 4 (pseudogene)	SYVN1	synovial apoptosis inhibitor 1, synoviolin
HSP90AA5P	heat shock protein 90kDa alpha (cytosolic), class A member 5	TACSTD1	tumor-associated calcium signal transducer 1

	(pseudogene)		
HSP90AA6P	heat shock protein 90kDa alpha (cytosolic), class A member 6 (pseudogene)	TAF4	TAF4 RNA polymerase II, TATA box binding protein (TBP)-associated factor, 135kDa
HSP90AB1	heat shock 90kDa protein 1, beta	TCEB1	transcription elongation factor B (SIII), polypeptide 1
HSP90AB2P	heat shock protein 90kDa alpha (cytosolic), class B member 2 (pseudogene)	TCEB2	transcription elongation factor B (SIII), polypeptide 2 (18kDa, elongin B)
HSP90AB3P	heat shock protein 90kDa alpha (cytosolic), class B member 3 (pseudogene)	TCLPA1	t-complex lethal Pa1
HSP90AB4P	heat shock protein 90kDa alpha (cytosolic), class B member 4 (pseudogene)	TCP1	t-complex 1
HSP90AB5P	heat shock protein 90kDa alpha (cytosolic), class B member 5 (pseudogene)	TFG	TRK-fused gene
HSP90AB6P	heat shock protein 90kDa alpha (cytosolic), class B member 6 (pseudogene)	TIAM1	T-cell lymphoma invasion and metastasis 1
HSP90B	heat shock protein hsp90 beta	TJP1	tight junction protein 1 (zona occludens 1)
HSP90B1	heat shock protein 90kDa beta (Grp94), member 1	TJP3	tight junction protein 3 (zona occludens 3)
HSP90B2P	heat shock protein 90kDa beta (Grp94), member 2 (pseudogene)	TMEM43	transmembrane protein 43
HSP90B3P	heat shock protein 90kDa beta (Grp94), member 3 (pseudogene)	TMOD3	tropomodulin 3 (ubiquitous)
HSPA14	heat shock 70kDa protein 14	TNPO3	transportin 3
HSPA1A	heat shock protein 1B; heat shock protein 1A; heat shock protein 1-like	TPBG	trophoblast glycoprotein
HSPA1B	heat shock protein 1B; heat shock protein 1A; heat shock protein 1-like	TPM3	tropomyosin 3
HSPA1L	heat shock protein 1B; heat shock protein 1A; heat shock protein 1-like	TPP1	Polynucleotide 3'-phosphatase
HSPA2	heat shock protein 2	TPT1	tumor protein, translationally-controlled 1
HSPA4	heat shock 70kDa protein 4	TRIM2	tripartite motif-containing 2
HSPA5	heat shock 70kDa protein 5 (glucose-regulated protein, 78kDa)	TRIP12	thyroid hormone receptor interactor 12

HSPA6	heat shock 70kDa protein 7 (HSP70B); heat shock 70kDa protein 6 (HSP70B')	TRN-SR	Transportin-Serine/Arginine rich
HSPA7	heat shock 70kDa protein 7 (HSP70B); heat shock 70kDa protein 6 (HSP70B')	TRO	trophinin
HSPA8	similar to Heat shock cognate protein 70	TROAP	trophinin associated protein
HSPA9	heat shock 70kDa protein 9 (mortalin)	TSG101	tumor susceptibility gene 101
HSPA9B	heat shock protein, 74 kDa, A	TTLL5	similar to tubulin tyrosine ligase-like family, member 5
HSPB1	heat shock protein 1	UBB	ubiquitin B
HSPB2	heat shock 27kDa protein 2	UBC	ubiquitin C
HSPBP1	hypothetical protein LOC100158355	UBE2D1	ubiquitin-conjugating enzyme E2D 1 (UBC4/5 homolog, yeast)
HSPD1	heat shock 60kDa protein 1 (chaperonin)	UBE2D2	ubiquitin-conjugating enzyme E2D 2 (UBC4/5 homolog, yeast)
HSPH1	heat shock 105kDa/110kDa protein 1	UBE2D3	ubiquitin-conjugating enzyme E2D 3 (UBC4/5 homolog, yeast)
IFI44	interferon-induced protein 44	UBE2E1	ubiquitin-conjugating enzyme E2E 1 (UBC4/5 homolog, yeast)
IL1RAPL1	interleukin 1 receptor accessory protein-like 1	UBE2J1	ubiquitin-conjugating enzyme E2, J1 (UBC6 homolog, yeast)
IL8	interleukin 8	UBE2J2	predicted gene 5801; ubiquitin-conjugating enzyme E2, J2 homolog (yeast)
IPO11	importin 11	UBE2L3	ubiquitin-conjugating enzyme E2L 3
IPO7	importin 7	UBE2L7P	ubiquitin-conjugating enzyme E2L 7 pseudogene
IPO9	Importin 9	UBE2N	ubiquitin-conjugating enzyme E2N (UBC13 homolog)
ITCH	itchy homolog E3 ubiquitin protein ligase (mouse)	UBE2V1	ubiquitin-conjugating enzyme E2 variant 1; transmembrane protein 189
KAB	KARP-1 binding protein 1	UBE3A	ubiquitin protein ligase E3A
KIF2A	kinesin family member 2A	UBE4A	ubiquitination factor E4A (UFD2 homolog)
KIF3A	kinesin family member 3A	UBE4B	ubiquitination factor E4B
KIF5B	kinesin family member 5B	USP9X	ubiquitin specific peptidase 9, X-linked
KIF5C	kinesin family member 5C	VCP	valosin-containing protein
KLC1	kinesin light chain 1	VPS4A	vacuolar protein sorting 4 homolog A (S. cerevisiae)
KLC3	kinesin light chain 3	VPS4B	vacuolar protein sorting 4B (yeast)
KPNB1	karyopherin (importin) beta 1	WFS1	Wolfram syndrome 1 (wolframin)
LGALS3	lectin, galactoside-binding, soluble, 3	WSB1	WD repeat and SOCS box-containing 1

LGALS4	lectin, galactoside-binding, soluble, 4	XPNPEP3	X-prolyl aminopeptidase (aminopeptidase P) 3, putative
LIMA1	LIM domain and actin binding 1	XPO1	exportin 1 (CRM1 homolog, yeast)
LIN7C	lin-7 homolog C (C. elegans)	ZCCHC16	zinc finger, CCHC domaincontaining 16
LMNA	lamin A/C	ZMYM2	zinc finger, MYM-type 2

Table S3. Enrichment significance for genes influencing CFTR biogenesis

Differentially expressed genes from the miR-138 mimic or SIN3A DsiRNA microarray experiment in Calu-3 cells were cross-referenced with the CFTR-Associated Gene Network (Fig. 3C). Fisher's Exact Test was used to generate an enrichment score for genes in the CFTR-Associated Gene Network from either one or both array datasets and referenced against the background (expressed genes with fold change <1.5 and *P* value >0.05).

	In CFTR-Associated Gene Network	Not in CFTR-Associated Gene Network	*P* value (Fisher's Exact Test)
Background gene list (20,019 genes)	196 (0.97%)	19,823	
Differentially expressed genes in the miR-138 mimic array (2,809 genes, *P* value <0.05)	73 (2.6%)	2,736	< 2.2e-16
Differentially expressed genes in the SIN3A DsiRNA array (2,840 genes, *P* value <0.05)	81 (2.9%)	2,759	< 2.2e-16
Intersection of differentially expressed genes in the miR-138 mimic and SIN3A DsiRNA array (773 genes, *P* value <0.05)	29 (3.8%)	744	1.269e-08

Table S4. Genes in the CFTR-Associated Gene Network identified as differentially expressed in Calu-3 cells following miR-138 or SIN3A DsiRNA treatment

The 125 genes in the CFTR-Associated Gene Network identified as differentially expressed in Calu-3 cells following treatment with SIN3A DsiRNA, miR-138 mimic, or negative control (Scr) (Fig. 3C). RNA was isolated from Calu-3 cells 48 hrs post-transfection for each experiment. The cellular compartments where each gene product has been demonstrated to function are indicated. The green shading indicates the 29 differentially expressed genes (Fig. 3C, SI Table S3) found by intersecting the SIN3A DsiRNA array, miR-138 mimic array, and the CFTR-Associated Gene Network. Orange shading indicates the 52 differentially expressed genes (Fig. 3C, SI Table S3) identified by intersecting the SIN3A DsiRNA array and the CFTR-Associated gene network. The blue shading denotes the 44 differentially expressed genes (Fig. 3C, SI Table S3) found by intersecting the miR-138 mimic array and the CFTR-Associated Gene Network. A literature survey identified that several of the differentially expressed gene products are known to influence CFTR protein biogenesis (references indicated). The microarray data are available from Genbank (accession no. XXXX).

	SCR vs SIN3A DsiRNA in Calu-3 cells				**SCR vs miR-138 mimic in Calu-3 cells**					
Gene Symbol	***P* value**	**q-value**	**Fold change**	**Description**	***P* value**	**q-value**	**Fold change**	**Description**	**Cellular compartment (29-31)**	**Evidence supporting a role in CFTR biogenesis**
AHSA1	1.61E-05	0.012531	-3.46199	SCR down vs SIN3A DsiRNA	0.019687	0.25731	-1.35164	SCR down vs miR-138 mimic	ER	Wang et al., 2006 (27)
AIFM1	0.0070715	0.15756	-1.25746	SCR down vs SIN3A DsiRNA	0.67482	0.77136	-1.01677	SCR down vs miR-138 mimic	Mitochondria	
AMFR	0.074739	0.34891	-1.11304	SCR down vs SIN3A DsiRNA	0.029462	0.30129	-1.1743	SCR down vs miR-138 mimic	ER	Okiyoneda et al., 2010 (16), Morito et al., 2008 (32)
ANO1	0.66474	0.6452	1.04484	SCR up vs SIN3A DsiRNA	0.018091	0.25129	-1.13876	SCR down vs miR-138 mimic	Cell membrane/	

									Cytoplasm	
ARF4	1.08E-07	0.0011043	11.2179	SCR up vs SIN3A DsiRNA	0.0026934	0.13638	2.14856	SCR up vs miR-138 mimic	Cytoplasm	
ARIH1	0.00030289	0.052976	-1.50153	SCR down vs SIN3A DsiRNA	0.018203	0.25141	-1.22173	SCR down vs miR-138 mimic	ER	
ATP2A2	0.45985	0.57562	-1.04296	SCR down vs SIN3A DsiRNA	4.01E-05	0.04964	-3.28909	SCR down vs miR-138 mimic	Membrane (ER)	
ATP6V1A	0.086870	0.36266	1.28326	SCR up vs SIN3A DsiRNA	0.023873	0.27584	1.37665	SCR up vs miR-138 mimic	Cytoplasm	Gomes-Alves et al., 2009 (28)
C6orf48	0.79852	0.68491	-1.01529	SCR down vs SIN3A DsiRNA	0.00094879	0.10264	-1.43339	SCR down vs miR-138 mimic		
CALU	0.0013256	0.082494	-1.85796	SCR down vs SIN3A DsiRNA	0.40333	0.68516	-1.11166	SCR down vs miR-138 mimic	ER	Gomes-Alves et al., 2010 (33), Riordan, 2008 (34)
CANX	2.48E-05	0.015913	2.48084	SCR up vs SIN3A DsiRNA	0.00027294	0.082131	-3.9665	SCR down vs miR-138 mimic	Membrane (ER)	Okiyoneda et al., 2002 ,(35), 2004 (36) Amaral, 2005 (37)
CAPNS1	0.00030013	0.052919	1.62708	SCR up vs SIN3A DsiRNA	0.011601	0.21325	1.50522	SCR up vs miR-138 mimic	Cytoplasm/ Cell membrane	Averna et al., 2011 (38)
CAPRIN1	0.021636	0.24574	-1.38596	SCR down vs SIN3A DsiRNA	0.32374	0.65203	-1.06328	SCR down vs miR-138 mimic	Cytoplasm/ membrane	
CBL	0.00073926	0.067941	-1.52704	SCR down vs SIN3A DsiRNA	0.21810	0.58825	-1.10291	SCR down vs miR-138 mimic	Cytoplasm	

CCT3	0.0079845	0.16647	1.06435	SCR up vs SIN3A DsiRNA	0.084007	0.43743	-1.05837	SCR down vs miR-138 mimic	Cytoplasm	Xu et al., 2006 (39)
CCT4	0.17258	0.43754	-1.11454	SCR down vs SIN3A DsiRNA	0.035947	0.32257	1.13169	SCR up vs miR-138 mimic	Cytoplasm	Xu et al., 2006 (39)
CD36	0.0012627	0.081077	1.26071	SCR up vs SIN3A DsiRNA	0.0083964	0.19056	-1.30301	SCR down vs miR-138 mimic	Membrane	
CD46	0.018465	0.23255	1.15585	SCR up vs SIN3A DsiRNA	0.018579	0.25287	1.2212	SCR up vs miR-138 mimic	Cytoplasm	
CD59	0.0083479	0.16854	-1.19037	SCR down vs SIN3A DsiRNA	0.0716399	0.41259	1.10033	SCR up vs miR-138 mimic	Cell membrane	
CDH1	0.047676	0.30860	1.09583	SCR up vs SIN3A DsiRNA	0.000527555	0.100395	1.61882	SCR up vs miR-138 mimic	Cell membrane	
CEP170	0.024747	0.25831	-2.0017	SCR down vs SIN3A DsiRNA	0.466766	0.70748	1.10426	SCR up vs miR-138 mimic	Cytoplasm	
CFL1	0.0011978	0.079843	-1.1756	SCR down vs SIN3A DsiRNA	0.124343	0.49675	1.09421	SCR up vs miR-138 mimic	Nucleus/ Cytoplasm	
CFTR	0.012744	0.19932	-1.50046	SCR down vs SIN3A DsiRNA	0.0354625	0.219467	-1.612486	SCR down vs miR-138 mimic	Cell membrane	
CLINT1	0.0021190	0.097838	-1.36507	SCR down vs SIN3A DsiRNA	0.107882	0.47518	-1.1829	SCR down vs miR-138 mimic	Cytoplasm/ Membrane	
COPB1	0.024636	0.25831	-1.47584	SCR down vs SIN3A DsiRNA	0.0695752	0.41045	-1.16536	SCR down vs miR-138 mimic	Cytoplasm/ Golgi	Rennolds et al., 2008 (40)
COPB2	0.023437	0.25289	-1.19889	SCR down vs SIN3A DsiRNA	0.689709	0.77324	-1.01608	SCR down vs miR-138 mimic	Cytoplasm/ Golgi	Rennolds et al., 2008 (40)
CSTB	0.65516	0.64286	1.02048	SCR up vs SIN3A DsiRNA	0.0169669	0.24604	-1.09972	SCR down vs miR-138 mimic	Cytoplasm/ Nucleus	
CYB5B	0.58292	0.61947	-1.0426	SCR down vs SIN3A DsiRNA	0.00411535	0.14967	1.195	SCR up vs miR-138 mimic	Mitochondria	
DAB2	0.0015343	0.08668	-1.79223	SCR down vs SIN3A DsiRNA	0.642821	0.76236	-1.03643	SCR down vs miR-138 mimic	Cytoplasmic vesicle/mem	Fu et al., 2011 (41)

									brane	
DERL1	0.0048852	0.13571	1.38671	SCR up vs SIN3A DsiRNA	0.00542543	0.16414	1.34459	SCR up vs miR-138 mimic	ER	Sun et al., 2006 (42)
DNAJA1	0.018151	0.23045	1.1753	SCR up vs SIN3A DsiRNA	0.287928	0.62985	1.12332	SCR up vs miR-138 mimic	Membrane(ER/Mitochondria)	Okiyoneda et al., 2010 (16)
DNAJA2	0.17775	0.44117	-1.27386	SCR down vs SIN3A DsiRNA	0.0144112	0.23249	-1.35192	SCR down vs miR-138 mimic	Membrane(ER/Mitochondria)	
DNAJB1	0.00467	0.13345	-1.3115	SCR down vs SIN3A DsiRNA	0.00620712	0.17200	-1.20906	SCR down vs miR-138 mimic	Cytoplasm/ Nucleus	Loo et al., 1998 (43)
DNAJB2	0.0054745	0.14277	-1.14103	SCR down vs SIN3A DsiRNA	0.00397351	0.14944	-1.29637	SCR down vs miR-138 mimic	ER	Okiyoneda et al., 2010 (16)
DNAJB4	0.93405	0.71790	1.0126	SCR up vs SIN3A DsiRNA	0.000600954	0.10160	-1.69113	SCR down vs miR-138 mimic	Cytoplasm/ Cell membrane	
DNAJB5	0.04355	0.30481	-1.16062	SCR down vs SIN3A DsiRNA	0.67625	0.77136	1.03618	SCR up vs miR-138 mimic	ER/cytoplasm	
DNAJC3	0.017765	0.22786	1.18253	SCR up vs SIN3A DsiRNA	0.34254	0.663	1.06795	SCR up vs miR-138 mimic	ER	
DNAJC5	0.021354	0.24515	-1.12525	SCR down vs SIN3A DsiRNA	0.61081	0.75450	-1.03939	SCR down vs miR-138 mimic	ER	
DPYSL2	0.0003101 2	0.052976	1.34553	SCR up vs SIN3A DsiRNA	0.82731	0.80259	-1.0083	SCR down vs miR-138 mimic	Cytoplasm	
DTL	0.0003001 3	0.052919	1.62708	SCR up vs SIN3A DsiRNA	0.011601	0.21325	1.50522	SCR up vs miR-138 mimic	Nucleus	
ERBB2	0.72939	0.66475	-1.02232	SCR down vs SIN3A DsiRNA	0.023092	0.27238	1.10719	SCR up vs miR-138 mimic	Cell membrane	
EXO1	0.047676	0.30860	1.09583	SCR up vs SIN3A DsiRNA	0.0005275 5	0.10039	1.61882	SCR up vs miR-138 mimic	Nucleus	
FN1	0.55651	0.61078	1.10482	SCR up vs SIN3A	0.047750	0.35996	-1.13802	SCR down vs	Secreted	

				DsiRNA				miR-138 mimic		
GNAI2	0.095517	0.37214	-1.13811	SCR down vs SIN3A DsiRNA	0.019199	0.25553	1.31869	SCR up vs miR-138 mimic	Membrane	
GNB2L1	0.0019162	0.094827	-1.19676	SCR down vs SIN3A DsiRNA	0.0048052	0.15668	1.08993	SCR up vs miR-138 mimic	Cell membrane	
HAX1	0.020490	0.24207	-1.09439	SCR down vs SIN3A DsiRNA	0.036990	0.32615	-1.10308	SCR down vs miR-138 mimic	Mitochondria/ER	
HSP90AA5P	0.46371	0.57693	-1.02053	SCR down vs SIN3A DsiRNA	0.004368	0.15289	1.13076	SCR up vs miR-138 mimic	Cytoplasm	
HSP90AB1	0.0070715	0.15756	-1.25746	SCR down vs SIN3A DsiRNA	0.67482	0.77136	-1.01677	SCR down vs miR-138 mimic	Cytoplasm	
HSP90AB4P	0.0036006	0.12180	1.29349	SCR up vs SIN3A DsiRNA	0.024902	0.28152	1.20176	SCR up vs miR-138 mimic	Cytoplasm/ER	
HSP90B1	0.019716	0.23852	-1.15306	SCR down vs SIN3A DsiRNA	0.30453	0.64101	-1.02907	SCR down vs miR-138 mimic	ER	
HSPA1A	0.36764	0.53808	1.03534	SCR up vs SIN3A DsiRNA	0.0066991	0.17773	-1.13272	SCR down vs miR-138 mimic	Cytoplasm	McLellan et al., 2005 (44)
HSPA1B	0.52318	0.59986	-1.02916	SCR down vs SIN3A DsiRNA	0.035042	0.31871	-1.22484	SCR down vs miR-138 mimic	ER	
HSPA5	0.0012627	0.081077	1.26071	SCR up vs SIN3A DsiRNA	0.0083964 7	0.19056	-1.30301	SCR down vs miR-138 mimic	ER	Okiyoneda et al., 2010 (16)
HSPA8	0.022036	0.46597	1.03953	SCR up vs SIN3A DsiRNA	0.032877	0.65556	1.02613	SCR up vs miR-138 mimic	ER	Okiyoneda et al., 2010 (16)
HSPH1	0.11651	0.39757	1.10934	SCR up vs SIN3A DsiRNA	0.036447	0.32411	1.0568	SCR up vs miR-138 mimic	ER	
IFI44	0.0033295	0.11829	-1.4303	SCR down vs SIN3A DsiRNA	0.0036995	0.14818	-1.17785	SCR down vs miR-138 mimic	Cytoplasm	
IL8	0.0012508	0.081077	-1.53641	SCR down vs SIN3A DsiRNA	0.27813	0.62365	-1.0325	SCR down vs miR-138 mimic	Secreted	

IPO7	0.021893	0.24628	-1.28697	SCR down vs SIN3A DsiRNA	0.66865	0.76925	-1.05573	SCR down vs miR-138 mimic	Cytoplasm/ Nucleus	
IPO9	0.41550	0.55856	1.08217	SCR up vs SIN3A DsiRNA	0.010336	0.20386	1.30339	SCR up vs miR-138 mimic	Nucleus	
KIF2A	0.0012508	0.081077	-1.53641	SCR down vs SIN3A DsiRNA	0.27813	0.62365	-1.0325	SCR down vs miR-138 mimic	Cytoplasm	
KIF3A	0.019187	0.23603	-1.69424	SCR down vs SIN3A DsiRNA	0.020133	0.25813	-1.66333	SCR down vs miR-138 mimic	Cytoplasm	
KLC1	0.022475	0.24879	-1.23103	SCR down vs SIN3A DsiRNA	0.27821	0.62367	-1.03394	SCR down vs miR-138 mimic	Cytoplasm	
LIN7C	0.029554	0.27188	-1.39075	SCR down vs SIN3A DsiRNA	0.023080	0.27238	-1.29217	SCR down vs miR-138 mimic	Cell Membrane	
MARCH3	0.18840	0.44829	1.10157	SCR up vs SIN3A DsiRNA	0.039927	0.33565	1.45175	SCR up vs miR-138 mimic	Membrane (ER, lysosome)	
MARCH5	0.027520	0.26590	-1.20855	SCR down vs SIN3A DsiRNA	0.046874	0.35684	-1.32176	SCR down vs miR-138 mimic	Membrane (Golgi)	
MARCH8	0.38424	0.54441	1.08064	SCR up vs SIN3A DsiRNA	0.0089270	0.19551	-1.26098	SCR down vs miR-138 mimic	Cytoplasmic vesicle membrane	
MARCH9	0.65156	0.64193	-1.01764	SCR down vs SIN3A DsiRNA	0.015383	0.23694	1.14263	SCR up vs miR-138 mimic	Membrane (ER, golgi, lysosome)	
MDM2	0.018896	0.23422	1.47227	SCR up vs SIN3A DsiRNA	0.88957	0.81411	1.00671	SCR up vs miR-138 mimic	ER	Okiyoneda et al., 2010 (16)
MUC13	0.029923	0.27280	1.27671	SCR up vs SIN3A DsiRNA	0.17301	0.55199	-1.1594	SCR down vs miR-138 mimic	Cell membrane/ Secreted	
NEDD4	0.15355	0.42657	-1.27145	SCR down vs SIN3A DsiRNA	0.0041411	0.14972	-1.57035	SCR down vs miR-138 mimic	Cytoplasm/ Cell membrane	Caohuy et al., 2009 (45)

NPEPPS	0.030349	0.27328	-1.17896	SCR down vs SIN3A DsiRNA	0.90233	0.81740	1.00816	SCR up vs miR-138 mimic	Cytoplasm/ Nucleus	
PARK7	0.055616	0.32245	-1.17228	SCR down vs SIN3A DsiRNA	0.032157	0.31007	1.07313	SCR up vs miR-138 mimic	Cytoplasm/ Nucleus/Mitochondria	Okiyoneda et al., 2010 (16)
PCMT1	0.027334	0.26525	1.22867	SCR up vs SIN3A DsiRNA	0.016646	0.24379	1.25673	SCR up vs miR-138 mimic	Cytoplasm	
PPP2CA	0.041791	0.30057	-1.15391	SCR down vs SIN3A DsiRNA	0.073160	0.41682	-1.08823	SCR down vs miR-138 mimic	Cytoplasm/ Nucleus	
PPP2CB	0.00073926	0.067941	-1.52704	SCR down vs SIN3A DsiRNA	0.21810	0.58825	-1.10291	SCR down vs miR-138 mimic	Cytoplasm/ Nucleus	
PPP2R1B	0.084944	0.36119	-1.04208	SCR down vs SIN3A DsiRNA	0.034627	0.31765	-1.10104	SCR down vs miR-138 mimic	Cytoplasm/ Nucleus	
PRKAB1	0.15856	0.42881	-1.08675	SCR down vs SIN3A DsiRNA	0.0098717	0.20080	-1.15418	SCR down vs miR-138 mimic	Cytoplasm/ mitochondria	
PRKAR2A	0.025070	0.25881	1.14948	SCR up vs SIN3A DsiRNA	0.97208	0.82740	1.00223	SCR up vs miR-138 mimic	ER/Golgi/ Cytoplasm	
PRKDC	0.46658	0.57825	1.0732	SCR up vs SIN3A DsiRNA	0.0098717	0.20080	1.4406	SCR up vs miR-138 mimic	Cytoplasm	
PSAP	0.044940	0.30552	-1.04209	SCR down vs SIN3A DsiRNA	0.11333	0.48211	-1.06961	SCR down vs miR-138 mimic	Lysosome	
PSENEN	0.024242	0.25718	1.18026	SCR up vs SIN3A DsiRNA	0.11785	0.48791	-1.06725	SCR down vs miR-138 mimic	Membrane (ER/Golgi)	
PSMA2	0.00255	0.10497	-1.33197	SCR down vs SIN3A DsiRNA	0.095343	0.45602	-1.14552	SCR down vs miR-138 mimic	Cytoplasm	
PSMB1	0.033826	0.28015	-1.17517	SCR down vs SIN3A DsiRNA	0.062900	0.39729	-1.1133	SCR down vs miR-138 mimic	Cytoplasm	
PSMB3	0.041791	0.30057	-1.15391	SCR down vs SIN3A DsiRNA	0.073160	0.41682	-1.08823	SCR down vs miR-138 mimic	Cytoplasm	
PSMB4	0.019716	0.23852	-1.15306	SCR down vs SIN3A DsiRNA	0.30453	0.64101	-1.02907	SCR down vs miR-138 mimic	Cytoplasm	Gomes-Alves et

										al., 2009 (28)
PSMC4	0.26540	0.49093	-1.05373	SCR down vs SIN3A DsiRNA	0.0012379	0.11199	-1.2333	SCR down vs miR-138 mimic	Cytoplasm	
PSMD2	0.27936	0.49685	-1.03903	SCR down vs SIN3A DsiRNA	0.0009343 7	0.10264	-1.22995	SCR down vs miR-138 mimic	Cytoplasm	
PSME2	0.0038616	0.12311	-1.28234	SCR down vs SIN3A DsiRNA	0.037191	0.32615	-1.05329	SCR down vs miR-138 mimic	Cytoplasm	Gomes-Alves et al., 2010 (33)
RANBP1	0.067280	0.33849	-1.14645	SCR down vs SIN3A DsiRNA	0.0098678	0.20080	1.17892	SCR up vs miR-138 mimic	Nucleus/ Cytoplasm	
RCN1	0.0004641 7	0.059638	1.532	SCR up vs SIN3A DsiRNA	0.91037	0.81870	-1.00768	SCR down vs miR-138 mimic	ER	Riordan, 2008 (34)
RCN2	0.54208	0.60607	1.07129	SCR up vs SIN3A DsiRNA	0.0044519	0.15405	1.51937	SCR up vs miR-138 mimic	ER	Riordan, 2008 (34)
RNF128	0.0099783	0.18386	1.29054	SCR up vs SIN3A DsiRNA	0.089316	0.44584	1.24366	SCR up vs miR-138 mimic	Endosome membrane	
RNF5	0.0014832	0.086337	-1.23699	SCR down vs SIN3A DsiRNA	0.59021	0.74898	-1.02225	SCR down vs miR-138 mimic	Membrane/ ER/ Mitochondria	
RPS27A	0.014817	0.20962	1.16618	SCR up vs SIN3A DsiRNA	0.019903	0.25736	-1.07778	SCR down vs miR-138 mimic	Ubiquitin: Cytoplasm/ Nucleus	
RUVBL1	0.031107	0.27492	-1.27252	SCR down vs SIN3A DsiRNA	0.95679	0.82533	-1.00192	SCR down vs miR-138 mimic	Nucleus	
RUVBL2	0.012273	0.19621	-1.25677	SCR down vs SIN3A DsiRNA	0.74289	0.78593	-1.01715	SCR down vs miR-138 mimic	Nucleus	
S100A6	0.10278	0.38125	-1.03031	SCR down vs SIN3A DsiRNA	0.040501	0.33761	-1.07952	SCR down vs miR-138 mimic	Nucleus/ Cytoplasm	
SAR1B	0.001534	0.086681	-1.79223	SCR down vs	0.64282	0.76236	-1.03643	SCR down vs	ER/Golgi	Yoo et al.,

	3			SIN3A DsiRNA				miR-138 mimic		2002 (46)
SEC31	0.014295	0.20631	-1.2903	SCR down vs SIN3A DsiRNA	0.36154	0.66781	1.10972	SCR up vs miR-138 mimic	Cytoplasm/ Cytoplasmic vesicle	Wang et al., 2004 (47), 2008 (48)
SEPT3	0.13198	0.41184	-1.2196	SCR down vs SIN3A DsiRNA	0.005846 4	0.16771	1.14975	SCR up vs miR-138 mimic	Cytoplasm	
SERP1	0.14214	0.41838	-1.08846	SCR down vs SIN3A DsiRNA	0.044318	0.34845	1.07253	SCR up vs miR-138 mimic	Membrane (ER)	Yamaguchi et al., 1999 (49)
SH3BG RL2	0.000780 09	0.069200	1.27715	SCR up vs SIN3A DsiRNA	0.36493	0.66974	1.05099	SCR up vs miR-138 mimic	Nucleus	
SHRO OM3	0.82982	0.692961	-1.01069	SCR down vs SIN3A DsiRNA	0.037189	0.32615	-1.12975	SCR down vs miR-138 mimic	Cell junction/ Cytoplasm	
SIN3A	0.000000 108	0.001104 3	11.2179	SCR up vs SIN3A DsiRNA	0.002693 4	0.13638	2.14856	SCR up vs miR-138 mimic	Nucleus	
SLC9A 2	0.54112	0.60556	1.05547	SCR up vs SIN3A DsiRNA	0.007090 6	0.18068	1.41754	SCR up vs miR-138 mimic	Cell membrane	
SLC9A 3R1	0.068323	0.3399	-1.08533	SCR down vs SIN3A DsiRNA	0.000493 57	0.10039	1.26929	SCR up vs miR-138 mimic	Cytoplasm/ Membrane protein	
SQRD L	0.017185	0.22378	-1.22939	SCR down vs SIN3A DsiRNA	0.14380	0.51993	-1.12326	SCR down vs miR-138 mimic	Mitochondri a	
ST13	0.005976	0.14845	-1.43969	SCR down vs SIN3A DsiRNA	0.35391	0.66668	1.05662	SCR up vs miR-138 mimic	Cytoplasm	
STIP1	0.030615	0.27442	-1.13552	SCR down vs SIN3A DsiRNA	0.97796	0.82787	1.00179	SCR up vs miR-138 mimic	Cytoplasm/ Nucleus	Okiyoneda et al., 2010 (16)
STX1A	0.95643	0.72231	-1.00117	SCR down vs SIN3A DsiRNA	0.049094	0.36341	-1.14888	SCR down vs miR-138 mimic	Cytoplasmic vesicle/Secr etory vesicle	

TCEB1	0.034431	0.28246	-1.11742	SCR down vs SIN3A DsiRNA	0.23671	0.59940	-1.05385	SCR down vs miR-138 mimic	Nucleus	
TCEB2	0.026312	0.26185	-1.12125	SCR down vs SIN3A DsiRNA	0.12352	0.49601	1.04679	SCR up vs miR-138 mimic	Nucleus	
TMEM43	0.022158	0.24720	-1.21214	SCR down vs SIN3A DsiRNA	0.33573	0.65964	-1.06038	SCR down vs miR-138 mimic	Nucleus	
TMOD3	0.051722	0.31560	-1.38236	SCR down vs SIN3A DsiRNA	0.037506	0.32671	-1.19026	SCR down vs miR-138 mimic	Cytoplasm	
TPM3	0.024909	0.25857	-1.10305	SCR down vs SIN3A DsiRNA	0.20200	0.57531	-1.06587	SCR down vs miR-138 mimic		
TPT1	0.056163	0.32308	-1.06789	SCR down vs SIN3A DsiRNA	0.037114	0.32615	-1.08914	SCR down vs miR-138 mimic	Cytoplasm	
TRIM2	0.033826	0.28015	-1.17517	SCR down vs SIN3A DsiRNA	0.062900	0.39729	-1.1133	SCR down vs miR-138 mimic	Cytoplasm	
TTLL5	0.11181	0.39142	-1.08133	SCR down vs SIN3A DsiRNA	0.0018652	0.12288	1.29484	SCR up vs miR-138 mimic	Cell projection/ Nucleus/ Cytoplasm	
UBC	0.0046730	0.13345	-1.31157	SCR down vs SIN3A DsiRNA	0.0062071	0.17200	-1.20906	SCR down vs miR-138 mimic	ER	Younger et al., 2004 (50)
UBE2D1	0.34893	0.53116	-1.06745	SCR down vs SIN3A DsiRNA	0.038136	0.32951	-1.19781	SCR down vs miR-138 mimic	Cytoplasm	Okiyoneda et al., 2010 (16)
UBE2E1	0.011802	0.19535	1.29504	SCR up vs SIN3A DsiRNA	0.91496	0.81920	1.00367	SCR up vs miR-138 mimic	Nucleus	
UBE2N	0.27748	0.49605	1.16888	SCR up vs SIN3A DsiRNA	0.017948	0.25036	-1.19433	SCR down vs miR-138 mimic	Nucleus/ Cytoplasm	Okiyoneda et al., 2010 (16)
UBE4B	0.41550	0.55856	1.08217	SCR up vs SIN3A DsiRNA	0.010336	0.20386	1.30339	SCR up vs miR-138 mimic	Cytoplasm	Okiyoneda et al., 2010 (16)

VPS4B	0.0064234	0.15287	-1.33358	SCR down vs SIN3A DsiRNA	0.0038640	0.14931	-1.28937	SCR down vs miR-138 mimic	Endosome membrane	
XPO1	0.88937	0.70679	-1.01945	SCR down vs SIN3A DsiRNA	0.0068479	0.17867	1.36536	SCR up vs miR-138 mimic	Cytoplasm/ Nucleus	

Table S5. Gene Ontology enrichment of genes co-regulated in Calu-3 cells following miR-138 mimic or SIN3A DsiRNA treatment

The 773 differentially expressed genes (Fig. 3C) found by intersecting the SIN3A DsiRNA array and the miR-138 mimic array, were subject to 'functional annotation clustering' using The Database for Annotation, Visualization and Integrated Discovery (DAVID)(51). Presented here are the top 15 enrichment clusters identified with a FDR <0.1. Each cluster is accompanied with the following information: enrichment score for the cluster, the number of genes, fold enrichment, and FDR.

Cluster	Term	# of genes	Fold Enrichment	FDR
1	**Enrichment Score: 6.373714295309155**			
	Chaperone	32	4.60	2.6E-09
	GO:0051082~unfolded protein binding	26	4.80	1.4E-07
	GO:0006457~protein folding	29	3.39	4.5E-05
	GO:0031072~heat shock protein binding	16	4.59	2.2E-03
	IPR015609:Molecular chaperone, heat shock protein, Hsp40, DnaJ	12	6.30	2.9E-03
	SM00271:DnaJ	12	5.67	7.0E-03
	domain:J	12	5.54	1.3E-02
	IPR001623:Heat shock protein DnaJ, N-terminal	12	5.38	1.5E-02
	IPR018253:Heat shock protein DnaJ, conserved site	12	5.27	1.9E-02
	IPR002939:Chaperone DnaJ, C-terminal	6	14.35	3.7E-02
2	**Enrichment Score: 6.25938918306378**			
	GO:0051789~response to protein stimulus	25	4.84	3.3E-07
	GO:0006986~response to unfolded protein	20	5.84	1.1E-06
	GO:0006984~ER-nuclear signaling pathway	12	7.10	7.7E-04
	GO:0034976~response to endoplasmic reticulum stress	11	6.70	5.2E-03
	GO:0034620~cellular response to unfolded protein	9	8.88	5.8E-03
	GO:0030968~endoplasmic reticulum unfolded protein response	9	8.88	5.8E-03
3	**Enrichment Score: 5.500411858307561**			
	endoplasmic reticulum	64	2.04	1.5E-04
	GO:0005783~endoplasmic reticulum	81	1.77	7.4E-04
4	**Enrichment Score: 4.989968351059494**			
	GO:0043161~proteasomal ubiquitin-dependent protein catabolic process	20	4.06	6.1E-04
	GO:0010498~proteasomal protein catabolic process	20	4.06	6.1E-04
	GO:0044265~cellular macromolecule catabolic process	65	1.86	3.2E-03
	GO:0051603~proteolysis involved in cellular protein catabolic process	56	1.93	5.5E-03
	GO:0044257~cellular protein catabolic process	56	1.92	6.5E-03
	GO:0030163~protein catabolic process	57	1.90	7.9E-03
	GO:0009057~macromolecule catabolic process	67	1.78	9.3E-03
	GO:0006511~ubiquitin-dependent protein catabolic process	30	2.57	9.9E-03

	GO:0043632~modification-dependent macromolecule catabolic process	53	1.91	1.4E-02
	GO:0019941~modification-dependent protein catabolic process	53	1.91	1.4E-02
5	**Enrichment Score: 4.675699610419189**			
	GO:0043161~proteasomal ubiquitin-dependent protein catabolic process	20	4.06	6.1E-04
	GO:0010498~proteasomal protein catabolic process	20	4.06	6.1E-04
	GO:0031396~regulation of protein ubiquitination	19	3.94	2.1E-03
	GO:0051340~regulation of ligase activity	17	4.35	2.3E-03
	GO:0051351~positive regulation of ligase activity	16	4.54	2.9E-03
	GO:0031397~negative regulation of protein ubiquitination	16	4.48	3.5E-03
	GO:0051436~negative regulation of ubiquitin-protein ligase activity during mitotic cell cycle	15	4.78	3.5E-03
	GO:0031145~anaphase-promoting complex-dependent proteasomal ubiquitin-dependent protein catabolic process	15	4.78	3.5E-03
	GO:0051444~negative regulation of ubiquitin-protein ligase activity	15	4.64	5.2E-03
	GO:0051352~negative regulation of ligase activity	15	4.64	5.2E-03
	GO:0051438~regulation of ubiquitin-protein ligase activity	16	4.25	6.9E-03
	GO:0051443~positive regulation of ubiquitin-protein ligase activity	15	4.44	8.9E-03
	GO:0044092~negative regulation of molecular function	37	2.29	9.1E-03
	GO:0006511~ubiquitin-dependent protein catabolic process	30	2.57	9.9E-03
	GO:0051439~regulation of ubiquitin-protein ligase activity during mitotic cell cycle	15	4.38	1.1E-02
	GO:0051247~positive regulation of protein metabolic process	30	2.56	1.1E-02
	GO:0031398~positive regulation of protein ubiquitination	16	3.95	1.8E-02
	GO:0031400~negative regulation of protein modification process	19	3.31	2.7E-02
	GO:0051437~positive regulation of ubiquitin-protein ligase activity during mitotic cell cycle	14	4.27	3.2E-02
	GO:0032270~positive regulation of cellular protein metabolic process	28	2.49	3.8E-02
	GO:0043086~negative regulation of catalytic activity	31	2.32	5.1E-02
	GO:0000278~mitotic cell cycle	37	2.07	8.5E-02
	GO:0032268~regulation of cellular protein metabolic process	44	1.92	8.6E-02
	GO:0032269~negative regulation of cellular protein metabolic process	23	2.65	9.8E-02
6	**Enrichment Score: 4.445439726104499**			
	GO:0043067~regulation of programmed cell death	75	1.91	1.2E-04
	GO:0010941~regulation of cell death	75	1.91	1.4E-04
	GO:0042981~regulation of apoptosis	74	1.91	1.8E-04
	GO:0043066~negative regulation of apoptosis	41	2.40	8.1E-04
	GO:0043069~negative regulation of programmed cell death	41	2.37	1.2E-03
	GO:0060548~negative regulation of cell death	41	2.36	1.3E-03
	GO:0006916~anti-apoptosis	26	2.61	3.5E-02

7	**Enrichment Score: 3.800565305189148**			
	GO:0043233~organelle lumen	125	1.44	2.3E-02
	GO:0070013~intracellular organelle lumen	122	1.43	3.3E-02
	GO:0031974~membrane-enclosed lumen	126	1.42	3.6E-02
8	**Enrichment Score: 3.7639457515427486**			
	nucleotide-binding	120	1.62	1.8E-04
	GO:0032553~ribonucleotide binding	123	1.42	4.7E-02
	GO:0032555~purine ribonucleotide binding	123	1.42	4.7E-02
	GO:0017076~purine nucleotide binding	127	1.41	5.6E-02
	GO:0000166~nucleotide binding	144	1.36	7.0E-02
	atp-binding	89	1.53	9.1E-02
9	**Enrichment Score: 3.5376428280629657**			
	GO:0033554~cellular response to stress	54	1.98	4.5E-03
	GO:0006974~response to DNA damage stimulus	39	2.17	1.9E-02
10	**Enrichment Score: 3.3100660934321877**			
	GO:0043232~intracellular non-membrane-bounded organelle	166	1.34	3.6E-02
	GO:0043228~non-membrane-bounded organelle	166	1.34	3.6E-02
11	**Enrichment Score: 3.196277550756004**			
	GO:0044427~chromosomal part	39	2.11	2.6E-02
	GO:0005694~chromosome	43	1.96	5.8E-02
12	**Enrichment Score: 3.0026983971129426**			
	GO:0046907~intracellular transport	58	1.83	2.0E-02
	GO:0006886~intracellular protein transport	38	2.10	4.7E-02
	GO:0034613~cellular protein localization	40	2.02	7.2E-02
	GO:0045184~establishment of protein localization	63	1.70	7.7E-02
	GO:0070727~cellular macromolecule localization	40	2.00	8.5E-02
13	**Enrichment Score: 2.7917083841293207**			
	GO:0010033~response to organic substance	67	1.93	5.8E-04
14	**Enrichment Score: 2.648776861425179**			
	IPR002939:Chaperone DnaJ, C-terminal	6	14.35	3.7E-02
15	**Enrichment Score: 2.041439746344019**			
	GO:0007049~cell cycle	73	1.95	9.2E-05

	GO:0022402~cell cycle process	57	2.09	3.7E-04
	GO:0000278~mitotic cell cycle	37	2.07	8.5E-02